J. Fluid Mech. (2000), *vol.* 422, *pp.* 249–280. Printed in the United Kingdom

On the long-term evolution of an intense localized divergent vortex on the beta-plane

By G. M. REZNIK[1], R. GRIMSHAW[2] AND E. S. BENILOV[3]

[1]P. P. Shirshov Institute of Oceanology, Moscow 11728, Russia

[2]Department of Mathematics, Monash University, Clayton, Victoria 3168, Australia

[3]Department of Mathematics and Statistics, University of Limerick, Ireland

(Received 28 April 1998 and in revised form 6 June 2000)

The evolution of an intense barotropic vortex on the β-plane is analysed for the case of finite Rossby deformation radius. The analysis takes into account conservation of vortex energy and enstrophy, as well as some other quantities, and therefore makes it possible to gain insight into the vortex evolution for longer times than was done in previous studies on this subject. Three characteristic scales play an important role in the evolution: the advective time scale T_a (a typical time required for a fluid particle to move a distance of the order of the vortex size), the wave time scale T_w (the typical time it takes for the vortex to move through its own radius), and the distortion time scale T_d (a typical time required for the change in relative vorticity of the vortex to become of the order of the relative vorticity itself). For an intense vortex these scales are well separated, $T_a \ll T_w \ll T_d$, and therefore one can consider the vortex evolution as consisting of three different stages. The first one, $t \leqslant T_w$, is dominated by the development of a near-field dipolar circulation (primary β-gyres) accelerating the vortex. During the second stage, $T_w \leqslant t \leqslant T_d$, the quadrupole and secondary axisymmetric components are intensified; the vortex decelerates. During the last, third, stage the vortex decays and is destroyed. Our main attention is focused on exploration of the second stage, which has been studied much less than the first stage. To describe the second stage we develop an asymptotic theory for an intense vortex with initially piecewise-constant relative vorticity. The theory allows the calculation of the quadrupole and axisymmetric corrections, and the correction to the vortex translation speed. Using the conservation laws we estimate that the vortex lifetime is directly proportional to the vortex streamfunction amplitude and inversely proportional to the squared group velocity of Rossby waves. For open-ocean eddies a typical lifetime is about 130 days, and for oceanic rings up to 650 days. Analysis of the residual produced by the asymptotic solution explains why this solution is a good approximation for times much longer than the expected formal range of applicability. All our analytical results are in a good qualitative agreement with several numerical experiments carried out for various vortices.

1. Introduction

It is clearly seen from numerous numerical, laboratory and analytical investigations that the evolution of an intense quasi-geostrophic localized vortex on a β-plane consists of three different stages (see § 2 for a quantitative analysis). During the first stage the development of a secondary dipole circulation (the so-called β-gyre) in the vicinity of the vortex plays a major role. To describe this mechanism we see that the

monopole, for instance a cyclone, induces a northward (southward) motion to the east (west) of itself. (Here and in what follows we use the northern hemisphere sign convention.) In accordance with the law for conservation of potential vorticity the β-effect generates anticyclonic (cyclonic) vorticity to the east (west) of the initial vortex, i.e. a dipole is generated. This vortex-by-vortex induction also takes place in the case when the nonlinear term in the governing equation is neglected, and can therefore be interpreted as the radiation of Rossby waves by the localized monopole. Thus one can say that the β-gyres are created by the near-field radiation of Rossby waves. In the presence of nonlinearity the β-gyres advect the vortex along the dipole axis. In turn the dipole is advected by the vortex, resulting in a turning of the dipole axis in the same sense as that of the vortex; that is, counterclockwise (clockwise) for a cyclone (anticyclone). Thus a cyclone (anticyclone) moves northwestward (southwestward) along a curved trajectory; the trajectory shape and the β-gyres structure are related to the strength and structure of the initial vortex.

This stage has been studied closely in the laboratory (e.g. Firing & Beardsley 1976) and in numerical experiments (e.g. McWilliams & Flierl 1979; Mied & Lindemann 1979; Fiorino & Elsberry 1989). On the analytical side, Reznik & Dewar (1994) calculated the β-gyres and the trajectory of an arbitrary axisymmetric non-divergent barotropic vortex. Llewellyn Smith (1997) developed an analogous theory for a non-localized vortex. However, for divergent vortices, only some special cases have proven to be tractable. For example, point vortices (Reznik 1992) and vortices with piecewise-uniform potential vorticity (Sutyrin & Flierl 1994) were successfully considered in a one-and-half layer model. Recently Reznik, Grimshaw & Sriskandarajah (1997) and Sutyrin & Morel (1997) investigated this stage in the stratified case (for layered models). (Here and in what follows we use the terms 'divergent' and 'non-divergent' with reference to quasi-geostrophic models with finite and infinite deformation radius R_d, respectively. Also, sometimes we use the term 'Rossby scale' instead of 'deformation radius'.)

Comparison of these analytical results with numerical simulations shows that even a simple model taking into account only the first azimuthal harmonics (the β-gyres) gives surprisingly good results when describing the vortex evolution for times far beyond the formal time of applicability for this model (e.g. Reznik & Dewar 1994; Sutyrin *et al.* 1994). The same conclusion follows from the numerical experiments by Ross & Kurihara (1992) using a model with a small number of azimuthal modes to calculate the trajectory of an intense non-divergent vortex. Obviously such models strongly distort the far-field radiated Rossby waves, and therefore one can assume that the vortex dynamics is determined mainly by the near-field processes for relatively long times which, in turn, can greatly simplify the theoretical description of the vortex evolution.

In the second stage the influence of the other azimuthal harmonics generated by wave radiation and nonlinearity has to be taken into account. This influence gradually reduces the vortex amplitude and in doing so decelerates the vortex motion (e.g. Reznik & Dewar 1994; Sutyrin *et al.* 1994). At the same time, changes to the relative vorticity of the vortex remain relatively small, so that the vortex amplitude exceeds the amplitude of the radiated field. In the final third stage, the vortex distortion becomes strong and its amplitude decreases to the background level, i.e. the vortex ceases to exist as a coherent structure.

The second stage (which obviously is of more interest than the third one) has been less well-studied, even numerically. The exception is the numerical study by Sutyrin *et al.* (1994) which will be discussed throughout this paper. There have been a few

attempts to describe this stage analytically for various types of eddies. All the theories that we are aware of are based on the assumption that in the course of time the vortex tends to some quasi-stationary state when its zonal velocity greatly exceeds the meridional one and the Rossby wave wake can be considered as resonantly excited. This means that the wake is calculated in a similar manner to the calculation of lee waves behind an obstacle in an eastward uniform zonal flow on the β-plane. The resulting lowest-order solution consists of an intense vortex and a low-amplitude wave wake. The time evolution of this system of a vortex and its associated wave wake is determined by solvability conditions for the next approximation. This approach was applied by Flierl to investigate the dynamics of a strongly nonlinear warm eddy (Flierl 1984), by Korotaev & Fedotov (1994) to study a non-divergent intense monopole, and by Flierl & Haines (1994) to explore the decay of an eastward moving dipole. A similar approach was used by McDonald (1998) to investigate the decay of intense cyclones by Rossby wave radiation.

Although these theories give qualitatively reasonable results, nevertheless there remain some important unanswered questions. First, there is no evidence (numerical or observational) that the wave field radiated by the vortex can be considered as quasi-resonant. This is certainly not the case for the non-divergent barotropic monopole since the meridional and zonal components of its translation speed are always of the same order (e.g. Fiorino & Elsberry 1989; Reznik & Dewar 1994; Korotaev & Fedotov 1994). The divergent quasi-geostrophic monopole does tend to a quasi-stationary state with predominantly zonal propagation but this state is a non-radiating one (see § 5 for more details).

Second, the quasi-resonant Rossby wave wake has infinite energy (see, for example, equation (23) from Flierl 1984). This is of no great importance when considering the flow around an obstacle, in which case the wake is terminated in fact by a transient front, which propagates away from the obstacle with the appropriate group velocity. Thus the infinite energy is a consequence of making a long-time quasi-steady approximation in the frame of reference of the obstacle. But a vortex does not behave like an obstacle in this respect: it loses energy when radiating Rossby waves and therefore cannot possess an infinite-energy wave wake. In fact, the system of vortex and waves conserves energy (unlike the flow around an obstacle) and hence at all times the total energy is finite. Of course, if the Rossby wave wake is close to being quasi-steady in the vicinity of the vortex then a quasi-steady solution can be sought to describe the vortex motion, which is produced mainly by the near-field processes. This would be possible, for example, if the vortex translation speed changes more slowly than the wave wake. However, the vortex motion is produced by the near-field part of the wave wake (β-gyres), and therefore the typical evolution times of the speed and wave wake are comparable.

Third, none of the theories cited above provides conservation of energy and enstrophy, which are particularly important for the second stage of the vortex development.

The questions addressed in this work are the following ones:

What are the durations of the main stages of the vortex evolution?

What is the mechanism of the vortex deceleration?

What is the lifetime of the vortex imposed by the conservation of energy and enstrophy?

Why does the 'naive' asymptotic solution which is the sum of the initial vortex and the β-gyres describe so well the vortex evolution far beyond the formal time of this solution's applicability?

Does any non-radiating state exist which the intense vortex tends to with increasing time?

To focus in detail on the last four questions in particular, we consider the model of an intense initial vortex with piecewise-constant relative vorticity, suggested by SF94. The paper is organised as follows. Section 2 contains a general characterization of the development stages of a quasi-geostrophic vortex on a β-plane. In § 3 we discuss some integral laws which are useful for understanding general features of the vortex evolution. The model of an intense divergent vortex with initially piecewise-constant relative vorticity is described in § 4. Section 5 is concerned mainly with properties of the β-gyres. The axisymmetric and quadrupole corrections important at later stages of the vortex evolution are discussed in § 6. The mechanism of the vortex deceleration is considered in § 7. The discussion of our results and concluding remarks are presented in § 8.

2. Vortex evolution stages

The basic equation for the model under consideration is the well-known equation for conservation of potential vorticity written in moving coordinates attached to the vortex centre,

$$\frac{\partial(\nabla^2\Psi - R_d^{-2}\Psi)}{\partial t} - U\frac{\partial(\nabla^2\Psi - R_d^{-2}\Psi)}{\partial x} - V\frac{\partial(\nabla^2\Psi - R_d^{-2}\Psi)}{\partial y} + \beta\frac{\partial\Psi}{\partial x} + J(\Psi, \nabla^2\Psi) = 0. \quad (2.1)$$

Here Ψ is the streamfunction, U and V are the zonal and meridional translation speeds respectively, x, y denote eastward and northward coordinates and t time; ∇^2 and J are Laplacian and Jacobian operators, while R_d is the Rossby scale. The initial state is assumed to be a localized axisymmetrical vortex, i.e.

$$\Psi(r, 0) = \Psi_0(r). \quad (2.2)$$

Let the initial vortex scale L be of the order of R_d and a typical orbital velocity be U_p. Then an appropriate non-dimensional version of the problem (2.1), (2.2) is conveniently written as

$$\frac{\partial}{\partial t}(\nabla^2\Psi - \Psi) + J(\Psi + \alpha U y - \alpha V x, \quad \nabla^2\Psi - \Psi) + \alpha\frac{\partial\Psi}{\partial x} = 0. \quad (2.3)$$

Here the advective time $T_a = R_d/U_p$ is used as a time scale and the vortex translational speed scale U_t is determined from the balance between the second, third, and fourth terms in (2.1) (physically, this balance means that the beta-effect forces the vortex to move), i.e.

$$U_t = \beta R_d^2 \quad (2.4)$$

(see also Reznik 1992; Reznik & Dewar 1994). The parameter α is equal to the ratio between the characteristic vortex translation speed U_t and the typical orbital velocity U_p, i.e.

$$\alpha = \frac{\beta R_d^2}{U_p}. \quad (2.5)$$

The problem (2.3), (2.2) should be closed by a definition of the vortex centre, which

is fixed in these coordinates; the translation speed depends on this definition (e.g. Reznik & Dewar 1994).†

We can produce three different time scales using the parameters β, U_p, L, namely

$$T_a = \frac{R_d}{U_p}, \quad T_w = \frac{1}{\beta R_d}, \quad T_d = \frac{U_p}{\beta^2 R_d^3}. \tag{2.6}$$

Only two of these scales are independent. Each of these scales has a clear physical meaning. The 'advective' scale T_a is a typical time required for a fluid particle to move a distance of the order of the vortex size. The 'wave' scale T_w is the typical time it takes for the vortex to move a distance equal to its own size.

To understand the meaning of the scale T_d we consider the law of potential vorticity conservation,

$$\Pi = Q + \beta y = \text{const for a fluid particle}, \tag{2.7a}$$

$$Q = \nabla^2 \Psi - R_d^{-2} \Psi, \tag{2.7b}$$

where Q is the relative vorticity. (Strictly speaking only the first term $\nabla^2\Psi$ in Q is the relative vorticity, the second term $-R_d^{-2}\Psi$ describes the vortex-tube stretching due to free surface changes. The term 'relative vorticity' as applied to Q is used only for brevity.) It readily follows from (2.7*a*) that the meridional drift L_y of the vortex produces the relative vorticity change $\Delta Q = -\beta L_y$. Since $Q = O(U_p/R_d)$, one can obtain that the quantity ΔQ becomes of the order of Q when

$$L_y = L_d = \frac{U_p}{\beta R_d}. \tag{2.8}$$

The typical time taken to travel a distance L_d is equal to (see (2.4))

$$\frac{L_d}{U_t} = \frac{U_p}{\beta^2 R_d^3} = T_d. \tag{2.9}$$

Thus the scale T_d is a typical time required for the vortex relative vorticity change to become of the order of the relative vorticity itself. It is natural to call T_d the 'distortion' time. Note that the real distortion time of a divergent vortex can substantially exceed T_d since the vortex meridional translation speed is significantly smaller than βR_d^2 (see below in § 5).

One can readily obtain that

$$\frac{T_w}{T_a} = \frac{1}{\alpha}, \quad \frac{T_d}{T_a} = \frac{1}{\alpha^2}, \quad \alpha = \frac{\beta R_d^2}{U_p}. \tag{2.10}$$

The crucial importance of the parameter α follows from dimensional analysis of the problem (2.1), (2.2), which is characterized by the dimensional parameters β, R_d, U_p, and L. Only two independent non-dimensional quantities can be produced using these parameters. It is convenient to choose $\alpha = \beta R_d^2/U_p$, $\delta = L/R_d$. In the rigid lid approximation $R_d = \infty, \delta = 0$, and the problem is characterized by the single parameter α (see e.g. Reznik & Dewar 1994; Llewellyn Smith 1997). For simplicity we assume here that the initial vortex size is equal to the Rossby scale, so that $L = R_d$. Then $\delta = 1$ and the problem (2.1), (2.2) is again characterized only by α. Note that the scales T_a, T_w, and T_d are obtained independent of each other from physical

† We note that formally the coordinate system is of no importance since knowing the solution in *any* coordinates we are able to calculate the track of any characteristic vortex point. However from a physical point of view it is preferable to use the coordinates attached to the vortex.

considerations and also that the fact that they are related by the simple relations (2.10) illustrates the importance of the parameter α.

If the vortex has a moderate amplitude, i.e. $\alpha = O(1)$, then all three time scales T_a, T_w, and T_d are of the same order. Physically this means that the vortex rotation, Rossby wave radiation, and the vorticity distortion proceed at the same rate, i.e. there is no particular stage at which one of these processes dominates over the other ones. That is why an analytical description of a moderate-amplitude vortex is an extremely difficult problem.

Fortunately, real atmospheric and oceanic eddies are, as a rule, highly nonlinear; their orbital velocities greatly exceed translation ones, and the parameter α is small,

$$\alpha \ll 1. \tag{2.11}$$

We proceed from the non-dimensional form (2.3) of the potential vorticity equation. Then the solution for an intense vortex can be sought in the following asymptotic form:

$$\Psi = \Psi_0(r) + \alpha\Psi_1(r,\theta,t) + \alpha^2\Psi_2(r,\theta,t) + \cdots, \tag{2.12a}$$

$$Q = Q_0(r) + \alpha q_1(r,\theta,t) + \alpha^2 q_2(r,\theta,t) + \cdots, \tag{2.12b}$$

where (r,θ) are polar coordinates with origin at the vortex centre. Expansions (2.12) express the physical fact that the typical dimensional times (2.6) are well separated under the condition (2.11),

$$T_a \ll T_w \ll T_d, \tag{2.13}$$

as follows from (2.10). The relationships (2.13) allow us to divide the intense vortex evolution into different stages.

At the very early stage, $t < 1$ (in dimensional terms, $t < T_a$) the simple axisymmetric rotation (the terms $\Psi_0(r), Q_0(r)$ in (2.12)) dominates and the influence of the β-effect can be neglected. At the second stage,

$$1 \leqslant t \leqslant \alpha^{-1}, \tag{2.14}$$

the β-gyres (terms $\alpha\Psi_1, \alpha q_1$ in (2.12)) develop, producing the vortex motion along some trajectory; the vortex evolution is described by the sum $\Psi_0(r) + \alpha\Psi_1(r,\theta,t)$ at this stage. In dimensional terms, (2.14) is $T_a \leqslant t < T_w$. At the third stage,

$$\alpha^{-1} \leqslant t < \alpha^{-2}, \tag{2.15}$$

the higher-order terms in (2.12) have to be taken into account. These terms produce a decay of the initial axisymmetric state and contribute to a decrease of the translation speed. In dimensional terms, (2.15) is $T_w \leqslant t < T_d$. At the final fourth stage, $t \geqslant \alpha^{-2}$ (in dimensional terms, $t \geqslant T_d$), the vortex distortion becomes strong and the asymptotic expansion (2.12) fails.

Thus one can expect that the asymptotic expansion (2.12) is applicable up to times

$$t < \alpha^{-2}, \tag{2.16}$$

or in dimensional terms, $t < T_d$. Of course the suggested scheme is a speculative one in many respects, and one of the aims of the paper is to verify it using the simplest possible model. Our main attention is focused on exploration of the poorly understood stage (2.15).

In the above considerations we assume the vortex scale L to be of the order of the Rossby scale R_d. One can readily generalize the estimations for T_a, T_w and T_d to the

cases of large ($L > R_d$), and small ($L < R_d$) vortices. For a large vortex we have

$$T_a = \frac{L}{U_p}, \quad T_w = \frac{L}{\beta R_d^2}, \quad T_d = \frac{U_p}{\beta^2 R_d^3}\frac{L}{R_d}, \tag{2.17}$$

i.e. the distortion time for the large vortex increases as the vortex size L increases, and exceeds the analogous time (2.9) for the vortex with $L \approx R_d$. The analogous scales for a small (non-divergent) vortex, which is of interest for atmospheric applications, can be written as

$$T_a = \frac{L}{U_p}, \quad T_w = \frac{1}{\beta L}, \quad T_d = \frac{U_p}{\beta^2 L^3}. \tag{2.18}$$

We see that, contrary to the preceding case, the distortion time of the non-divergent vortex is very sensitive to the vortex size, decreasing proportionally to L^3 with increasing L. Obviously the difference between large and small eddies is related to the fact that with increasing wavelength λ, the group velocity of divergent Rossby waves decreases whereas the group velocity of non-divergent Rossby waves rapidly increases (proportionally to λ^2). In this paper, most attention is paid to the case of a divergent vortex with a scale L of the order of R_d.

The distortion times (2.9), (2.17), and (2.18) can be written in the following 'universal' form:

$$T_d = \frac{\Psi_m}{c_g^2}, \tag{2.19}$$

where Ψ_m is a typical vortex streamfunction amplitude ($\Psi_m = U_p L$), and the typical group velocity c_g is equal to βR_d^2 and βL^2 for the cases of finite and infinite Rossby scale, respectively. Note that (2.19) can also be written as

$$c_g T_d = \frac{U_p L}{c_g} \tag{2.20}$$

where the left-hand side is the distance moved by a Rossby wave in a time T_d, while the right-hand side is the product of U_p (the typical orbital velocity) with the time L/c_g in which a Rossby wave propagates across the vortex.

3. Integral quantities

In this Section various integral quantities are presented which enable us to understand some general properties of the long-term vortex evolution. Although all of them are well-known we present them here for convenience, noting that some of them are somewhat modified, being written in moving coordinates.

3.1. *Energy and enstrophy conservation*

Multiplying (2.3) by $\Psi (Q = \nabla^2 \Psi - \Psi)$ and integrating throughout the plane we obtain the energy (enstrophy) conservation law:

$$\int [(\nabla \Psi)^2 + \Psi^2] \mathrm{d}x\mathrm{d}y - \int \Psi Q \mathrm{d}x\mathrm{d}y = E_0 = \text{const}, \tag{3.1}$$

$$\int Q^2 \mathrm{d}x\mathrm{d}y = N_0 = \text{const}. \tag{3.2}$$

Substitution of (2.12) into (3.1), (3.2) gives the equations, at different powers of α,

$$-\int \Psi_0 Q_0 \, \mathrm{d}x\mathrm{d}y = E_0, \quad \int Q_0^2 \, \mathrm{d}x\mathrm{d}y = N_0, \tag{3.3a, b}$$

$$\int (\Psi_0 q_1 + \Psi_1 Q_0)\mathrm{d}x\mathrm{d}y = 0, \quad \int Q_0 q_1 \mathrm{d}x\mathrm{d}y = 0, \tag{3.4a, b}$$

$$\int (\Psi_2 Q_0 + \Psi_0 q_2)\mathrm{d}x\mathrm{d}y + \int \Psi_1 q_1 \mathrm{d}x\mathrm{d}y = 0, \quad 2\int Q_0 q_2 \mathrm{d}x\mathrm{d}y + \int q_1^2 \mathrm{d}x\mathrm{d}y = 0. \tag{3.5a, b}$$

Equations (3.3a, b) are trivial and (3.4a, b) are satisfied identically since Ψ_1 (β-gyres) always has the form

$$\Psi_1 = A_{s1}(r, t)\sin\theta + A_{c1}(r, t)\cos\theta. \tag{3.6}$$

The most useful equations are (3.5a) and (3.5b) relating the β-gyre energy and enstrophy (the second integrals in (3.5a, b), respectively) to the energy and enstrophy changes of the axisymmetric vortex component (first integrals in (3.5a, b) respectively). This enables one to calculate the energy and enstrophy lost by the initial vortex using only the beta-gyre correction Ψ_1, without solving the much more complicated problem for the correction Ψ_2.

3.2. *Moment equations*

Integrating (2.3) throughout the plane we obtain the equation

$$\int \Psi \mathrm{d}x\mathrm{d}y = -\int Q\mathrm{d}x\mathrm{d}y = M_0 = \text{const}, \tag{3.7}$$

which can be interpreted as angular momentum conservation.

Multiplication of (2.3) by (x, y) along with the subsequent integration gives the equations for the vortex centroid velocities:

$$\frac{\mathrm{d}}{\mathrm{d}t}\int x\Psi \mathrm{d}x\mathrm{d}y = -\alpha(U+1)\int \Psi \mathrm{d}x\mathrm{d}y, \quad \frac{\mathrm{d}}{\mathrm{d}t}\int y\Psi \mathrm{d}x\mathrm{d}y = -\alpha V \int \Psi \mathrm{d}x\mathrm{d}y. \tag{3.8a, b}$$

Note that in fixed coordinates the centroid velocity coincides with the drift velocity $(-1, 0)$. It readily follows from (3.8a, b), (3.7) that the centroid location is defined as follows:

$$\int x\Psi \mathrm{d}x\mathrm{d}y = -\alpha M_0 \bar{X}(t), \quad \int y\Psi \mathrm{d}x\mathrm{d}y = -\alpha M_0 \bar{Y}(t), \tag{3.9a, b}$$

where

$$\bar{X}(t) = \int_0^1 (U+1)\mathrm{d}t, \quad \bar{Y}(t) = \int_0^1 V\mathrm{d}t \tag{3.10}$$

are the zonal and meridional vortex displacements in coordinates moving with the drift velocity $(-1, 0)$.

To derive equations for the second moments we multiply (2.3) by (x^2, y^2, xy) and integrate the resulting equation. After some algebra we have

$$W_\Psi = \int (x^2 + y^2)(\Psi - \Psi_0)\mathrm{d}x\mathrm{d}y = \alpha^2 M_0(\bar{X}^2 + \bar{Y}^2), \tag{3.11a}$$

or, in alternative form,

$$W_Q = \int (x^2 + y^2)(Q - Q_0)\mathrm{d}x\mathrm{d}y = -\alpha^2 M_0(\bar{X}^2 + \bar{Y}^2). \tag{3.11b}$$

Here $Q_0 = \nabla^2\Psi_0 - \Psi_0$ is the initial relative vorticity.

Other equations for the second moments are written as

$$\frac{\mathrm{d}}{\mathrm{d}t}\left[\int xy\Psi \mathrm{d}x\mathrm{d}y - \alpha^2 M_0 \bar{X}\,\bar{Y}\right] = \int \left[\left(\frac{\partial\Psi}{\partial x}\right)^2 - \left(\frac{\partial\Psi}{\partial y}\right)^2\right]\mathrm{d}x\mathrm{d}y, \tag{3.12a}$$

$$\frac{\mathrm{d}}{\mathrm{d}t}\left[\int (x^2-y^2)\Psi\,\mathrm{d}x\mathrm{d}y-\alpha^2 M_0(\bar{X}^2-\bar{Y}^2)\right]=-4\int\frac{\partial\Psi}{\partial x}\frac{\partial\Psi}{\partial y}\mathrm{d}x\mathrm{d}y. \tag{3.12b}$$

Equations (3.12*a*, *b*) were used to control our numerical calculations. We emphasize that all formulae of this Section (excluding, of course, (3.3) to (3.5)) are exact and do not depend on the magnitude of α.

4. Intense vortex with initially piecewise-constant relative vorticity

We proceed from the non-dimensional form (2.3) of the equations. Let the initial relative vorticity be

$$Q_0=\nabla^2\Psi_0-\Psi_0=H(1-r), \tag{4.1}$$

where $H(z)$ is the Heaviside function: $H(z)=1$ if $z>0$ and $H(z)=0$ if $z<0$. The potential vorticity $\Pi=Q+\alpha y$ is equal to, at $t=0$,

$$\Pi=\Pi_0=H(1-r)+\alpha y. \tag{4.2}$$

By the conservation of potential vorticity the discontinuity in the right-hand side of (4.2) is conserved in time, i.e. the potential vorticity can be represented as

$$\Pi=Q+\alpha y \tag{4.3a}$$

where the relative vorticity

$$Q=\nabla^2\Psi-\Psi=H(r_b-r)+\alpha q(x,y,t). \tag{4.3b}$$

Here $q(x,y,t)$ is a continuous function and the patch boundary depends on θ and t so that

$$r_b=r_b(\theta,t). \tag{4.4}$$

Substituting (4.3*a*, *b*), (4.4) into (2.3) and equating to zero the singular and regular parts in the resulting equation we obtain

$$\frac{\partial q}{\partial t}+\frac{\partial\Psi}{\partial\theta}+J(\Psi^*,q)=0, \tag{4.5a}$$

$$\frac{\partial r_b}{\partial t}+\frac{1}{r_b}\frac{\partial\Psi^*}{\partial r}\bigg|_b\frac{\partial r_b}{\partial\theta}+\frac{1}{r_b}\frac{\partial\Psi^*}{\partial\theta}\bigg|_b=0, \tag{4.5b}$$

where

$$\Psi^*=\Psi+\alpha(Uy-Vx), \tag{4.5c}$$

and $a|_b=a(r_b,\theta,t)$. The third equation is (4.3*b*) and relates the streamfunction Ψ to the relative vorticity. The initial conditions are that

$$\Psi(r,\theta,0)=\Psi_0(r),\quad \nabla^2\Psi_0-\Psi_0=H(1-r), \tag{4.6a}$$

$$q(r,\theta,0)=0, \tag{4.6b}$$

and

$$r_b(\theta,0)=1. \tag{4.6c}$$

To close the problem we have to define a method to calculate the translation speed $\boldsymbol{U}=(U,V)$. The simplest way is to trace the centroid of the vortex patch $\boldsymbol{S}$† bounded

† It does not coincide with the vortex centroid, the location of which is determined by (3.8), (3.9).

by the curve $r = r_b(\theta, t)$. The centroid location (x_c, y_c) is given by the equations

$$x_c = \frac{\int_S x\mathrm{d}x\mathrm{d}y}{\int_S \mathrm{d}x\mathrm{d}y}, \quad y_c = \frac{\int_S y\mathrm{d}x\mathrm{d}y}{\int_S \mathrm{d}x\mathrm{d}y}, \tag{4.7}$$

which in polar coordinates take the form

$$x_c = \frac{1}{3S_0}\int_0^{2\pi} r_b^3(\theta,t)\cos\theta\mathrm{d}\theta, \quad y_c = \frac{1}{3S_0}\int_0^{2\pi} r_b^3(\theta,t)\sin\theta\mathrm{d}\theta. \tag{4.8}$$

Here

$$S_0 = \int_S \mathrm{d}x\mathrm{d}y = \frac{1}{2}\int_0^{2\pi} r_b^2(\theta,t)\mathrm{d}\theta = \text{constant} \tag{4.9}$$

is the area of the patch $\boldsymbol{S}$. Conservation of S_0 readily follows from (4.5b) rewritten as

$$\frac{\partial}{\partial t}\left(\frac{r_b^2}{2}\right) + \frac{\partial}{\partial\theta}\{\Psi^*[r_b(\theta),\theta]\} = 0. \tag{4.10}$$

In moving coordinates attached to the centroid $x_c = y_c = 0$, i.e. by (4.8) we have the equations

$$\int_0^{2\pi} r_b^3(\theta,t)\cos\theta\mathrm{d}\theta = 0, \quad \int_b^{2\pi} r_b^3(\theta,t)\sin\theta\mathrm{d}\theta = 0 \tag{4.11}$$

which close the problem (4.5), (4.6).

In the limit (2.11) of an intense vortex the solution is sought in the form (2.12); that is,

$$\Psi = \Psi_0(r) + \alpha\Psi_1(r,\theta,t) + \cdots, \tag{4.12a}$$

$$q = q_1(r,\theta,t) + \alpha q_2(r,\theta,t) + \cdots, \tag{4.12b}$$

$$r_b = 1 + \alpha\bar{r}_1(\theta,t) + \alpha^2\bar{r}_2(\theta,t) + \cdots, \tag{4.12c}$$

$$(U,V) = (U_0,V_0) + \alpha(U_1,V_1) + \cdots. \tag{4.12d}$$

When solving (4.5) we demand that $\Psi, \nabla\Psi$ are continuous on the curve $r = r_b(\theta,t)$ to provide the continuity of the pressure and velocity field.

The model under consideration was suggested by Sutyrin & Flierl (1994) in a somewhat different form. The exceptions are the important equations (4.11) which allow us to examine analytically higher-order terms in the expansions (4.12a–d) (the first-order quantities were found in Sutyrin & Flierl 1994) which are of importance at later stages of the vortex evolution. It may appear that this model is much more complicated than the original problem (2.1), (2.2) but this is not the case. The great simplification is that equation (4.5a) for the vorticity perturbation q does not contain the advection of the lowest-order vorticity $H(r_b - r)$; the advection is described instead by equation (4.5b).

5. The lowest-order solution and β-gyres

Substitution of (4.12a–d) into (4.3b), (4.5a, b) and (4.6) gives, at the lowest order,

$$\nabla^2\Psi_0 - \Psi_0 = H(1-r), \tag{5.1a}$$

$$[\Psi_0] = \left[\frac{\partial\Psi_0}{\partial r}\right] = 0, \tag{5.1b}$$

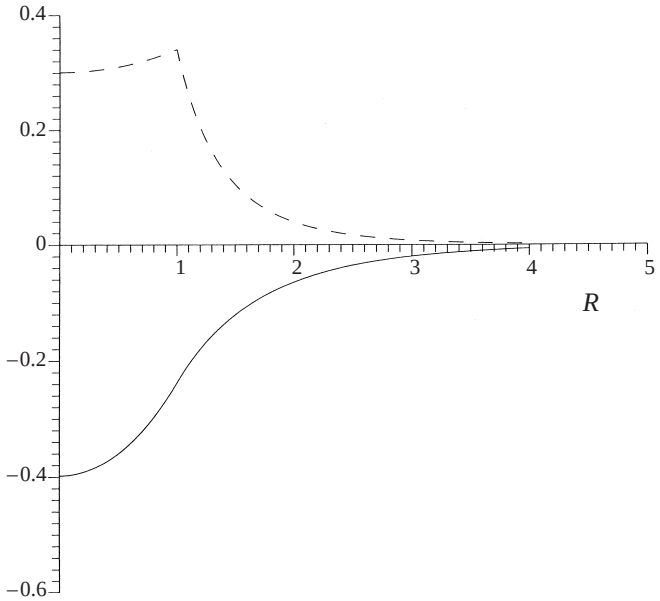

FIGURE 1. Radial profiles of the initial streamfunction $\Psi_0(r)$ (solid) and the angular velocity $\bar{\Omega}(r) = (1/r)\ \mathrm{d}\Psi_0/\mathrm{d}r$ (dashed).

$$\frac{\partial q_1}{\partial t} + \bar{\Omega}(r)\frac{\partial q_1}{\partial \theta} + r\bar{\Omega}(r)\cos\theta = 0, \tag{5.1c}$$

$$q_1(r,\ \theta,\ 0) = 0. \tag{5.1d}$$

Here $\bar{\Omega}(r)$ is the angular velocity of the initial vortex, that is

$$\bar{\Omega}(r) = \frac{1}{r}\frac{\partial \Psi_0}{\partial r}, \tag{5.2}$$

and the notation $[a] = a(1-0,\theta,t) - a(1+0,\theta,t)$ is used.

The initial streamfunction $\Psi_0(r)$ and $\bar{\Omega}(r)$ have the form

$$\Psi_0 = \begin{cases} -1 + K_1(1)I_0(r), & r \leqslant 1 \\ -I_1(1)K_0(r), & r > 1, \end{cases} \tag{5.3}$$

$$\bar{\Omega}(r) = \frac{1}{r}\begin{cases} K_1(1)I_1(r), & r \leqslant 1 \\ I_1(1)K_1(r), & r > 1, \end{cases} \tag{5.4}$$

where $K_n(r), I_n(r)$ are the modified Bessel functions of order n. The profiles of $\Psi_0(r)$ and $\bar{\Omega}(r)$ are shown in figure 1.

The vorticity correction q_1 is readily obtained from (5.1c) and has the dipolar form

$$q_1 = q_{1s}\sin\theta + q_{1c}\cos\theta, \tag{5.5a}$$

where

$$Q_1 = q_{1s} + \mathrm{i}q_{1c} = -r(1 - \exp(-\mathrm{i}\bar{\Omega}t)). \tag{5.5b}$$

For the first-order quantities we have

$$\nabla^2\Psi_1 - \Psi_1 = q_1(r,\theta,t), \tag{5.6a}$$

$$[\Psi_1] = 0, \quad \left[\frac{\partial \Psi_1}{\partial r}\right] = -\bar{r}_1(\theta,t), \tag{5.6b}$$

$$\frac{\partial \bar{r}_1}{\partial t} + \bar{\Omega}(1)\frac{\partial \bar{r}_1}{\partial \theta} + \frac{\partial \Psi_1(1,\theta,t)}{\partial \theta} + U_0\cos\theta + V_0\sin\theta = 0, \tag{5.6c}$$

$$\int_0^{2\pi} \bar{r}_1(\theta,t)\,\exp(\mathrm{i}\theta)\mathrm{d}\theta = 0, \tag{5.6d}$$

$$\frac{\partial q_2}{\partial t} + \bar{\Omega}(r)\frac{\partial q_2}{\partial \theta} = -J(\Psi_1 + U_0 y - V_0 x, q_1) - \frac{\partial \Psi_1}{\partial x}. \tag{5.6e}$$

Note that the discontinuities at $r = 1$ (see (5.6*b*) and analogous equations below) arise when writing at the non-perturbed patch boundary $r = 1$ the continuity condition of Ψ, $\nabla\Psi$ at $r = r_b(\theta, t)$.

The problem (5.6*a–d*) is solved by decomposition into a Fourier series in θ. As a result we have

$$\bar{r}_1(\theta,t) = 0, \tag{5.7a}$$

$$\Psi_1 = A_{s1}(r,t)\sin\theta + A_{c1}(r,t)\cos\theta, \tag{5.7b}$$

$$\frac{\partial \Psi_1(1,\theta,t)}{\partial \theta} + U_0\cos\theta + V_0\sin\theta = 0, \tag{5.7c}$$

where

$$A = A_{s1} + \mathrm{i}A_{c1} = -I_1(r)\int_r^\infty \xi Q_1 K_1(\xi)\mathrm{d}\xi - K_1(r)\int_0^r \xi Q_1 I_1(\xi)\mathrm{d}\xi, \tag{5.8}$$

and Q_1 is given by (5.5*b*). The translation speed components U_0, V_0 are obtained from (5.7*c*) and can be written as

$$U_0 + \mathrm{i}V_0 = -A^*(1,t) = -1 + I_1(1)\int_1^\infty \xi^2 K_1(\xi)\exp(\mathrm{i}\bar{\Omega}t)\mathrm{d}\xi + K_1(1)\int_0^1 \xi^2 I_1(\xi)\exp(\mathrm{i}\bar{\Omega}t)\mathrm{d}\xi. \tag{5.9}$$

Thus this lowest-order approximation describes the developing β-gyres (the function Ψ_1 in (5.7*b*)) advecting the vortex northwestward (see figures 2, 3) with the translation speed $\boldsymbol{U} = (U_0, V_0)$ given by (5.9); the vortex patch shape remains unchanged. The solution (5.5*a*, *b*), (5.7*a–c*), (5.9) was derived in Sutyrin & Flierl (1994) (with slightly different notation).† Here we consider some important properties of the beta-gyres Ψ_1 which were not analysed in Sutyrin & Flierl (1994).

Figure 2 shows a typical development of the beta-gyres gradually amplifying and expanding, with a broadening large-scale approximately rectilinear flow forming in the central region. The β-gyre magnitude increases very slowly with increasing time as can be seen in figure 2. The asymptotic behaviour of A for $u = \bar{\Omega}(r)t$ fixed, $t \to \infty$, is

$$A = \ln\tilde{t}[1 + F(u)] + O(1), \tag{5.10a}$$

$$F(u) = -\frac{u}{2}\int_u^\infty \frac{\mathrm{e}^{-\mathrm{i}v}}{v^2}\mathrm{d}v - \mathrm{i}\frac{\mathrm{e}^{-\mathrm{i}u} - 1}{2u}, \tag{5.10b}$$

where $\tilde{t} = I_1(1)t$ (see the Appendix).

The central flow advecting the vortex along the dipole axis appears to be practically uniform in some region near the vortex centre as readily follows from the behaviour of the residual flow Ψ_{res},Ψ_{res}

$$\Psi_{res} = \Psi_1 + U_0 y - V_0 x = [A_{s1}(r,t) - rA_{s1}(1,t)]\sin\theta + [A_{c1}(r,t) - rA_{c1}(1,t)]\cos\theta, \tag{5.11a}$$

† When comparing our results with Sutyrin & Flierl one should keep in mind that their non-dimensional time differs from ours, our $T = 100$ corresponds to their $T = 35$.

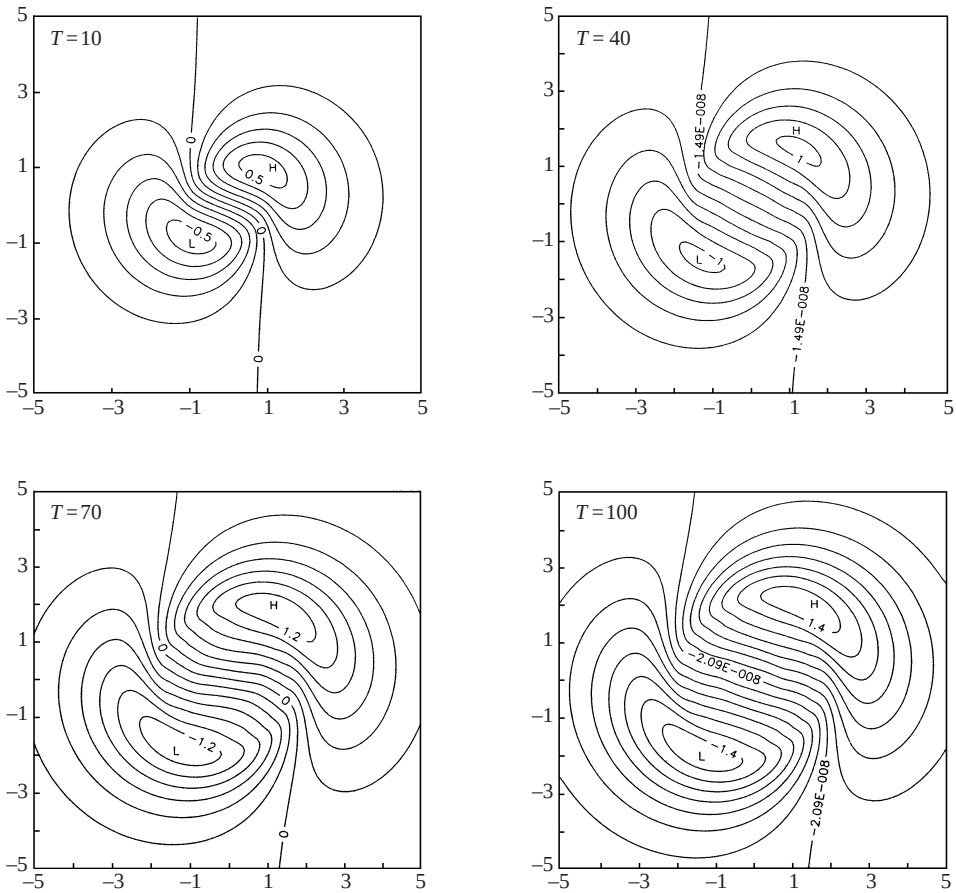

FIGURE 2. Development of the primary β-gyres.

shown in figure 4. It is clearly seen that Ψ_{res} practically vanishes in some region $r < r_{res}(t)$ centred at the vortex centre, i.e.

$$\Psi_{res} = \Psi_1 + U_0 y - V_0 x \approx 0, \quad r < r_{res}(t). \tag{5.11b}$$

The size (somewhat arbitrary) $r_{res}(t)$ of this region monotonically increases with increasing time: $r_{res}(50) \approx 1$, $r_{res}(100) \approx 2$. So, as time passes, the region becomes larger than the vortex patch.

This feature can be explained using the asymptotics of Ψ_1, U_0, V_0 for large times. For r fixed, and t large, we have

$$A = r + I_1(r)G(t) + O(1/t), \tag{5.12a}$$

$$\operatorname{Re} G(t) = -\frac{3\pi}{2}\frac{\ln^2 \tilde{t}}{\tilde{t}} + O(\ln \tilde{t}/\tilde{t}), \tag{5.12b}$$

$$\operatorname{Im} G(t) = \frac{\ln^3 \tilde{t}}{\tilde{t}} + \frac{3C \ln^2 \tilde{t}}{t} + O(\ln \tilde{t}/\tilde{t}), \tag{5.12c}$$

and

$$U_0 - \mathrm{i}V_0 = -A(1,t) = -1 + I_1(1)G(t) + O(1/t), \tag{5.13}$$

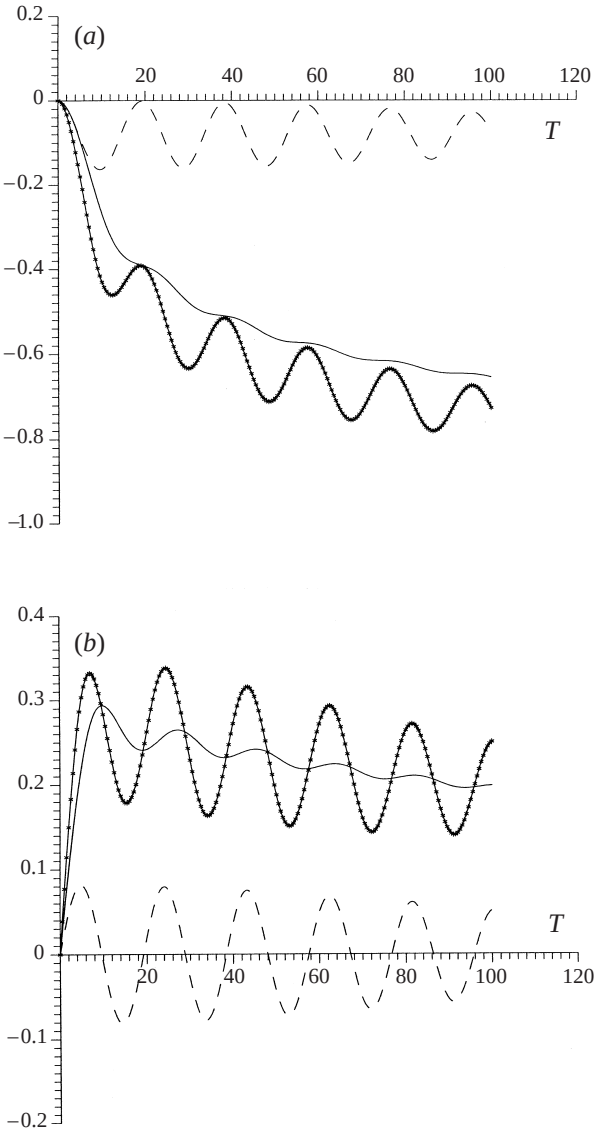

FIGURE 3. The lowest-order translation speed components: (*a*) zonal component U_0, (*b*) meridional component V_0. The oscillations of the speed in time are produced by the integral over the vortex patch region (the last term in (5.9)). The components U_0, V_0 (bold lines with stars) are decomposed into parts due to the last term (dashed lines), and the first two terms (thin solid lines) in (5.9). Almost solid-body rotation of the main vortex inside the vortex patch (see figure 1) results in a very slow decay of the oscillations in time.

where C is the Euler constant and we recall that $\tilde{t} = I_1(1)t$. By virtue of (5.12) and (5.7*b*) we now see that $\Psi_1 \to r\sin\theta$ in the region $r = O(1)$, $U_0 \to -1$ and $V_0 \to 0$ with increasing time. Therefore, the residual flow $\Psi_{res} \to 0$ in the region $r = O(1)$, which gradually expands with time. In accordance with (5.12*b*, *c*) this tendency is rather slow, much slower than that seen in figure 4. However, numerical calculations show that the asymptotics for (5.12*b*, *c*) are applicable only for very large times and the function G decreases much more rapidly than in (5.12) with increasing time for

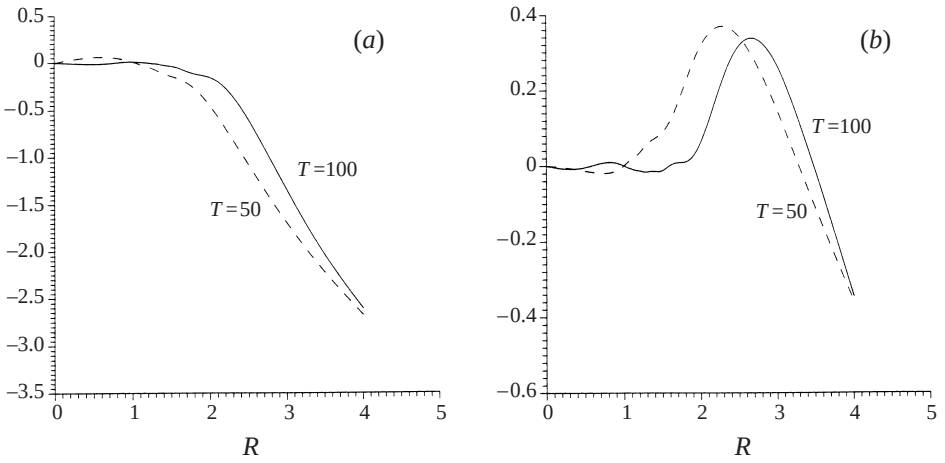

FIGURE 4. Radial profiles of the coefficients in (5.11*a*): (*a*) the coefficient $A_{s1}(r,t) - rA_{s1}(1,t)$; (*b*) the coefficient $A_{c1}(r,t) - rA_{c1}(1,t)$.

$t < 200$. In addition, one can write in the region $r = O(1)$,

$$A(r,t) - rA(1,t) = [I_1(r) - rI_1(1)]G(t) + O(1/t).$$

In practice, the difference $I_1(r) - rI_1(1)$ is small for r in the range $0 < r < 2$ and this also greatly contributes to the rapid residual flow decay in this region for moderate times ($t > 10$) as shown in figure 4. Note that the smallness of the residual flow $\Psi_1 + U_0 y - V_0 x$ in the main vortex region is observed in practice in all numerical experiments with localized vortices (e.g. Fiorino & Elsberry 1989).

The smallness of the residual flow is of great importance for understanding of the long-term vortex evolution because it has significant implications for the range of time over which the expansions (4.12) remain a good approximation to the solution. To show that, we consider the remainder arising when substituting the approximate solution $\Psi_0 + \alpha\Psi_1$ into the basic equation (2.3). The main part of this remainder is equal to the right-hand side of equation (5.6*e*) multiplied by α^2. The most 'dangerous' part of this remainder is the Jacobian containing the spatial derivatives of q_1 growing proportionally to t with increasing t (see (5.5)) and therefore one would expect a rapid growth of the remainder with time, resulting in a rapid loss of validity of the expansions (4.12). Instead, using (5.12), (5.5) one can show that formally the remainder grows proportionally to $\ln^3 t$ for large t. However, due to the exponential decay of Ψ_0 and, therefore, of q_1, the region of rapid growth is concentrated near the vortex centre where the growth is compensated by the smallness of Ψ_{res} in the Jacobian. This effect, together with the slow time growth of Ψ_1, results in a very slow increase of the right-hand side of (5.6*e*) with increasing time. Our calculations show that the right-hand side does not exceed 1.5 for $t = 100$. The boundedness of this remainder means that the approximate solution $\Psi_0 + \alpha\Psi_1$ can be a good approximation for many turnaround times exceeding the wave time T_w. This conclusion is confirmed by numerical experiments performed for various initial vortices in divergent (Sutyrin *et al.* 1994, their figure 4) and non-divergent (Reznik & Dewar 1994, their figures 1 to 3) models. Obviously, the behaviour of the right-hand side of (5.6*e*) retards the growth of the second vorticity correction q_2, which also contributes to a greater 'longevity' of the expansions (4.12). For analogous reasons the next-order remainder also does not grow catastrophically with increasing time (see the end of § 7).

It follows from (5.7*b*), (5.12), and (5.13) that *locally* the approximate solution $\Psi_0 + \alpha\Psi_1$ tends to

$$\bar{\Psi}_\infty = \Psi_0\left(\sqrt{(x+\alpha t)^2 + y^2}\right) + \alpha y \quad \text{as} \quad t \to \infty. \tag{5.14}$$

The state $\tilde{\Psi}_\infty$ is an exact solution to the equation (2.3) (with $U = V = 0$) for an arbitrary axisymmetric function $\Psi_0(r)$. One can say that the transformation (5.14) 'kills' the β-effect, which is why an arbitrary axisymmetric vortex moving with the drift velocity on the background of a uniform zonal flow with the same velocity does not radiate any Rossby waves. The tendency of the solution to the state (5.14) can be considered as an interesting example of a transient nonlinear self-organization when the nonlinearity and near-field radiated Rossby waves (the β-gyres) create the tendency for the vortex to adopt a non-radiating state and in doing so retard the vortex decline. Of course, this tendency holds only when the vortex is sufficiently strong.

6. The axisymmetric and quadrupole corrections

Taking into account (5.7*a*) the second-order approximation is described as follows:

$$\nabla^2\Psi_2 - \Psi_2 = q_2(r,\ \theta,\ t), \tag{6.1a}$$

$$[\Psi_2] = 0, \quad \left[\frac{\partial\Psi_2}{\partial r}\right] = -\bar{r}_2(\theta,\ t), \tag{6.1b}$$

$$\frac{\partial\bar{r}_2}{\partial t} + \bar{\Omega}(1)\frac{\partial\bar{r}_2}{\partial\theta} + \frac{\partial\Psi_2(1,\theta,t)}{\partial\theta} + U_1\cos\theta + V_1\sin\theta = 0, \tag{6.1c}$$

$$\int_0^{2\pi}\bar{r}_2(\theta,t)\exp(\mathrm{i}\theta)\mathrm{d}\theta = 0, \tag{6.1d}$$

$$\frac{\partial q_3}{\partial t} + \bar{\Omega}(r)\frac{\partial q_3}{\partial\theta} = -J(\Psi_1 + U_0 y - V_0 x, q_2) - J(\Psi_2 + U_1 y - V_1 x, q_1) - \frac{\partial\Psi_2}{\partial x}. \tag{6.1e}$$

As can be seen from (5.6*e*) the β-gyres self-interaction, β-effect, and advection of q_1 induce an axisymmetric and quadrupole components in the vorticity field, i.e. q_2 has the form,

$$q_2 = q_{20}(r,t) + q_{2s}(r,t)\sin 2\theta + q_{2c}(r,t)\cos 2\theta. \tag{6.2}$$

Here

$$q_{20} = \mathrm{Im}\int_0^t \frac{1}{2r}(\bar{A}^*\bar{Q}_1)'\mathrm{d}t - \int_0^t V_0\mathrm{d}t, \tag{6.3a}$$

$$q_{2s} + \mathrm{i}q_{2c} = \frac{1}{2r}\mathrm{e}^{-2\mathrm{i}\bar{\Omega}t}\int_0^t\left(\bar{A}\bar{Q}_1' - \bar{A}'\bar{Q}_1\right)\mathrm{e}^{2\mathrm{i}\bar{\Omega}t}\mathrm{d}t, \tag{6.3b}$$

$$\bar{A} = \bar{A}_{s1} + \mathrm{i}\bar{A}_{c1} = A(r,t) - rA(1,t), \tag{6.3c}$$

$$\bar{Q}_1 = \bar{q}_{1s} + \mathrm{i}\bar{q}_{1c} = r\mathrm{e}^{-\mathrm{i}\bar{\Omega}t}, \tag{6.3d}$$

where the prime denotes differentiation with respect to r. The streamfunction Ψ_2 and the patch boundary disturbance $\bar{r}_2$ are obtained from (6.1*a*) to (6.1*d*) using a decomposition into Fourier series and can be written as

$$\Psi_2 = B_{20}(r,t) + \bar{B}_{2s}(r,t)\sin 2\theta + \bar{B}_{2c}(r,t)\cos 2\theta, \tag{6.4a}$$

$$\bar{r}_2(\theta,t) = r_{2s}^{(2)}(t)\sin 2\theta + r_{2c}^{(2)}(t)\cos 2\theta, \tag{6.4b}$$

where

$$B_{20}(r,t) = -I_0(r)\int_r^\infty rK_0(r)q_{20}\mathrm{d}r - K_0(r)\int_0^r rI_0(r)q_{20}\mathrm{d}r, \tag{6.5a}$$

$$\bar{B}_2 = \bar{B}_{2s} + \mathrm{i}\bar{B}_{2c} = B_2 - R_2^{(2)}(t)\Phi(r), \tag{6.5b}$$

$$B_2(r,t) = -I_2(r)\int_r^\infty rK_2(r)(q_{2s}+\mathrm{i}q_{2c})\mathrm{d}r - K_2(r)\int_0^r rI_2(r)(q_{2s}+\mathrm{i}q_{2c})\mathrm{d}r, \tag{6.5c}$$

$$R_2^{(2)}(t) = r_{2s}^{(2)} + \mathrm{i}r_{2c}^{(2)} = -2\mathrm{i}\mathrm{e}^{\mathrm{i}\omega t}\int_0^t B_2(1,t)\mathrm{e}^{\mathrm{i}\omega t}\mathrm{d}t, \tag{6.5d}$$

$$\omega = 2\left[\bar{\Omega}(1) - \Phi_2(1)\right], \quad \Phi_2(r) = \begin{cases} K_2(1)I_2(r), & r < 1 \\ I_2(1)K_2(r), & r \geqslant 1. \end{cases} \tag{6.5e}$$

Since neither Ψ_2 nor $\bar{r}_2$ contain $\cos\theta$, $\sin\theta$ we have from (6.1*c*),

$$U_1 = V_1 = 0, \tag{6.6}$$

i.e. the translation velocity remains unchanged at this order.

The time evolution of the axisymmetric correction q_{20} is shown in figure 5. In accordance with potential vorticity conservation (2.7*a*) q_{20} is negative in a region around the vortex centre. As the vortex travels along the meridian this region becomes wider and 'deeper' giving rise to a broadening annulus in the field $Q_0 + \alpha^2 q_{20}$ with vorticity opposite in sign to the main vortex. The vorticity in the annulus has a fine structure, clearly seen in figure 5, with scale decreasing with increasing time because of the relatively rapid differential rotation in the main vortex for the range $1 \leqslant r \leqslant 2$ (see figure 1). One can expect that such a structure exists only in the absence of friction, which if included in the model would result in homogenization of the vorticity inside the annulus.

The formation of an annulus with oppositely signed vorticity was qualitatively predicted by Korotaev (e.g. Korotaev 1988) and demonstrated in numerical experiments (Sutyrin *et al.* 1994; Korotaev & Fedotov 1994). Somewhat more surprising is that this annulus is not alone; it is followed by two broadening annulae with alternating signs. We emphasize also that q_{20} is of the same sign as Q_0 at the vortex periphery, i.e. the angle-averaged relative vorticity increases with increasing time far from the vortex centre. It is important to note that the behaviour of q_{20} is qualitatively the same as the behaviour of the azimuthally averaged perturbation vorticity in the case of a non-divergent vortex examined numerically by Smith, Weber & Kraus (1995, see figure 2 of their paper). Therefore one might expect that these features are typical for vortex evolution on a β-plane.

The general features of the vorticity evolution described above are in a full agreement with the conservation laws (3.7), (3.11*b*). By virtue of (3.7) the integral W_Q in (3.11*b*) is always opposite in sign to the total angular momentum, i.e. is positive (negative) for a cyclone (anticyclone). The main contribution to W_Q is from the vortex periphery because of the multiplier r^2 in the integrand. Therefore the difference $Q-Q_0$ is, on average, positive for a cyclone and negative for an anticyclone on the vortex periphery, i.e. the vortex periphery always intensifies. On the other hand we have from (3.7) that

$$\int (Q - Q_0)\mathrm{d}x\mathrm{d}y = 0, \tag{6.7}$$

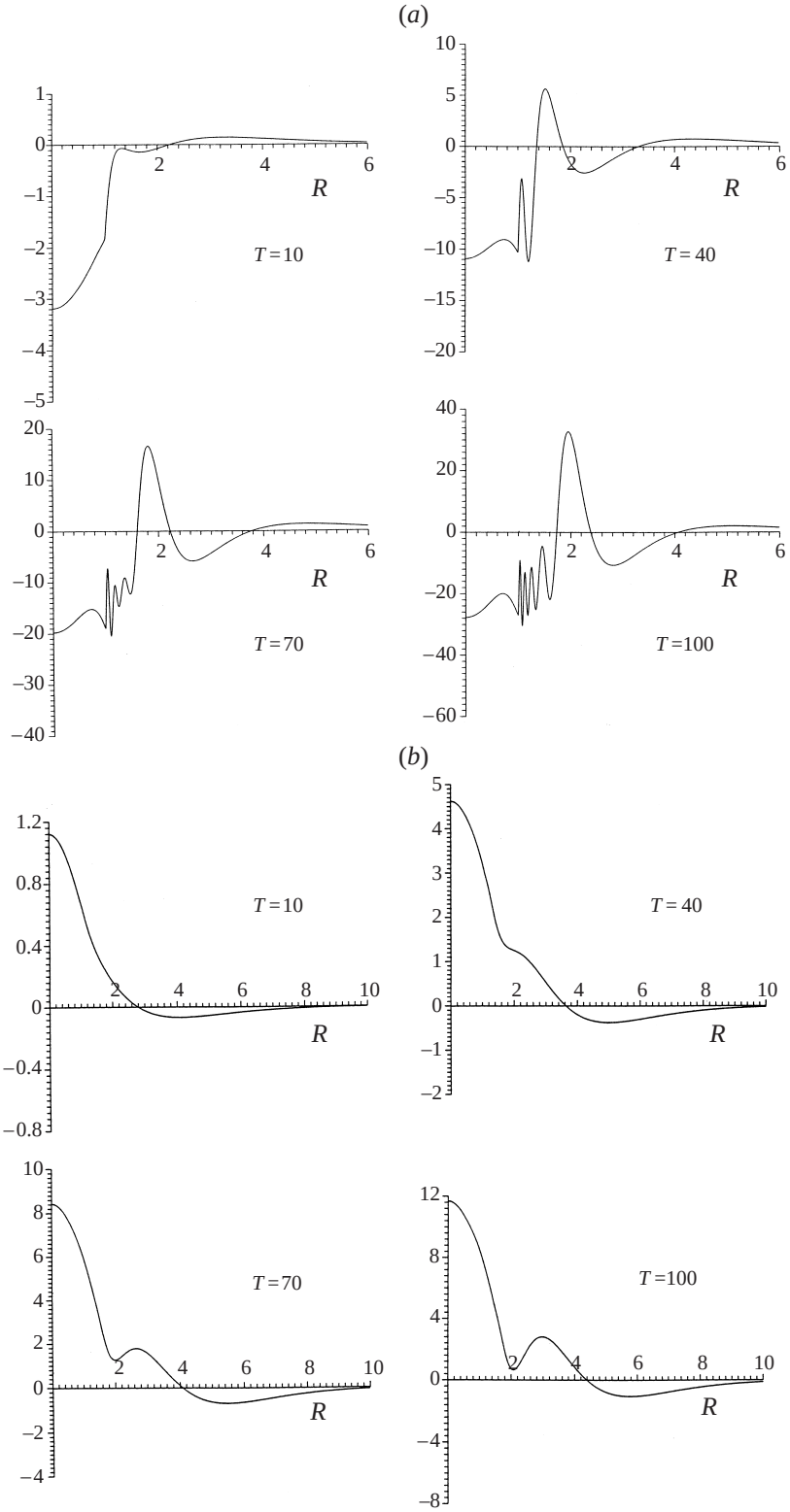

FIGURE 5. Radial profiles of the secondary axisymmetrical fields: (*a*) relative vorticity q_{20}; (*b*) streamfunction Ψ_{20}.

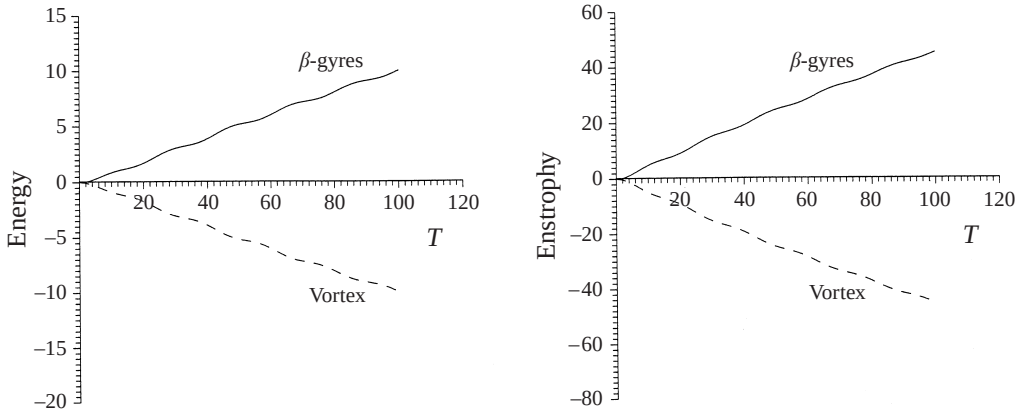

FIGURE 6. The non-dimensional energy and enstrophy (divided by $\alpha^2\pi$) gained by the beta-gyres and lost by the axisymmetric component.

whence it follows that for a cyclone (anticyclone) the positive (negative) difference $Q - Q_0$ on the vortex periphery has to be compensated by the negative (positive) difference $Q - Q_0$ in a central region. Thus the localized vortex weakens in the central region and intensifies at the periphery, i.e. it gradually broadens and 'flattens'. The integral W_Q in (3.11*b*), which can be considered as a measure of this flattening, is directly proportional to the squared distance travelled by the vortex in a frame moving with the drift velocity $(-1, 0)$. It readily follows from (5.12*b*, *c*), (5.13) that for the present case of an intense vortex the right-hand side of (3.11*b*) is dominated by the meridional displacement $\bar{Y}$ at large times,

$$W_Q = O(\ln^6 t), \quad t \gg 1. \tag{6.8}$$

At the same time in the linear case (i.e. when the nonlinear terms in (2.1) are omitted) the meridional speed of a linear vortex is equal to zero and the zonal speed is about 30% of the drift speed of -1 (Flierl 1977). Correspondingly, in the linear case, the integral W_Q grows proportionally to t^2, i.e. much faster than for the intense vortex. Thus a linear vortex expands much faster than a strongly nonlinear one which clearly demonstrates the 'self-binding' effect revealed in the numerical experiments by (McWilliams & Flierl 1979; Smith & Reid 1982; Horton 1989). The axisymmetric streamfunction correction B_{20} is much smoother than q_{20} and is approximately opposite in sign (see figure 5 and (3.11*a*)). Otherwise the behaviour of these fields is very similar to each other.

Knowing B_{20}, q_{20} one can check that the conservation laws (3.5*a*, *b*) are obeyed by the asymptotic solution (see figure 6). The total energy E_{ax} and enstrophy N_{ax} of the axisymmetric component are given by the equations

$$E_{ax} = E_0 - \alpha^2 E_\beta(t), \tag{6.9}$$

$$N_{ax} = N_0 - \alpha^2 N_\beta(t), \tag{6.10}$$

where

$$E_\beta(t) = -\int \Psi_1 q_1 \mathrm{d}x\mathrm{d}y = -\pi \int_0^\infty r(A_{s1}q_{1s} + A_{c1}q_{1c})\mathrm{d}r, \tag{6.11}$$

$$N_\beta(t) = \pi \int_0^\infty r|Q_1|^2 \mathrm{d}r \tag{6.12}$$

are the energy and enstrophy of the β-gyres, and E_0, N_0 are the total energy and enstrophy,

$$E_0 = -\int \Psi_0 Q_0 \mathrm{d}x\mathrm{d}y = -2\pi \int_0^1 r\Psi_0 \mathrm{d}r = 2\pi[\tfrac{1}{2} - K_1(1)I_1(1)] \approx 0.16 \times 2\pi, \quad (6.13a)$$

$$N_0 = \int Q_0^2 \mathrm{d}x\mathrm{d}y = \pi. \quad (6.13b)$$

Surprisingly, the time dependences of $E_\beta(t)$, $N_\beta(t)$ are remarkably well approximated by straight lines despite the rather complicated behaviour of the functions Ψ_1, q_1 (see figure 6). With a good accuracy the functions $\alpha^2 E_\beta(t)$, $\alpha^2 N_\beta(t)$ can be represented as

$$\alpha^2 E_\beta(t) = 2\pi \times 0.1\alpha^2 t = 0.2\pi \frac{t^*}{T_d}, \quad (6.14)$$

$$\alpha^2 N_\beta(t) = 0.45\pi \frac{t^*}{T_d}, \quad (6.15)$$

where t^* is the dimensional time, T_d is the distortion time. One can define the typical lifetime t_{lf}^E (t_{lf}^N) of the vortex as a time when the energy (enstrophy) of the axisymmetric component becomes equal to the energy of β-gyres, i.e.

$$E_{ax} = \alpha^2 E_\beta = \tfrac{1}{2} E_0 \quad (N_{ax} = \alpha^2 N_\beta = \tfrac{1}{2} N_0). \quad (6.16)$$

Taking into account (6.13a, b) we have that

$$t_{lf}^E = 0.8\, T_d \quad (t_{lf}^N = 1.1\, T_d). \quad (6.17)$$

These estimates are close to the distortion time T_d, thus confirming the self-consistency of our theory since the estimates for the lifetimes t_{lf}^E, t_{lf}^N and the estimate for the distortion time T_d are obtained in very different ways. At the same time the 'enstrophy' lifetime t_{lf}^N slightly exceeds the 'energy' lifetime t_{lf}^E. Physically it means that the vortex vorticity field distorts somewhat slower than the vortex velocity field, which is dominated by larger space scales and therefore is distorted faster by Rossby wave radiation. This effect was clearly seen in numerical experiments with a non-divergent vortex by Reznik & Dewar (1994): the relative vorticity extremum value decreased significantly slower than the streamfunction extremum value. One might expect that an analogous effect takes place for the divergent model.

For typical oceanic parameters in midlatitudes $\beta = 2 \times 10^{-13}\,\mathrm{cm^{-1}\,s^{-1}}$, $R_d = 45\,\mathrm{km}$ and the drift velocity $\beta R_d^2 \approx 4\,\mathrm{cm\,s^{-1}}$. The typical maximum swirl velocity in mid-oceanic eddies $U_p = 20\,\mathrm{cm\,s^{-1}}$ which corresponds here to $\alpha = 0.4\beta R_d^2/U_p = 0.08$.† Thus we have the following estimate for the 'energy' lifetime of mid-oceanic eddies,

$$t_{lf}^{mo} \approx 130 \text{ days}. \quad (6.18)$$

For rings with typical swirl velocity $1\,\mathrm{m\,s^{-1}}$,

$$t_{lf}^{r} \approx 650 \text{ days}. \quad (6.19)$$

Although rather crude (the energy losses caused by the higher azimuthal harmonics are not taken into account) the estimates (6.18), (6.19) are very reasonable and

† The non-dimensional maximum orbital velocity in our model is equal to 0.4 (see figure 1). Thus to fit the model vortex to a vortex with maximum orbital velocity U_p one should choose the parameter α in our model equal to $\alpha = 0.4\beta R_d^2/U_p$.

suggest that the energy transfer from the axisymmetric component to the β-gyres plays a substantial role in the vortex decay.

The time evolution of the second-order correction fields (6.2), (6.4*a*) is shown in figures 7 and 8. At the initial stage ($t = 10$) the streamfunction Ψ_2 looks like a tripole consisting of a distorted and elongated central anticyclone, and two weaker side cyclones. With time the distortion gradually grows due to the differential (fast in the central region and slow in the periphery) counterclockwise rotation of the main vortex. The structure that develops consists of a strong, practically axisymmetric central vortex surrounded by four weaker azimuthally elongated vortex satellites with alternating signs. The system expands and intensifies with increasing time, the satellite centres gradually migrating radially outward rather than rotating around the main vortex centre. Comparing figure 7(*a*) with figures 5(*b*), 8 one can readily see that the axisymmetric component B_{20}, and the harmonics $\sin 2\theta$ and $\cos 2\theta$ in (6.4*a*) are responsible for the central vortex and the satellite cyclones and anticyclones respectively. An important feature of this structure is that the quadrupole component $\bar{B}_{2s} \sin 2\theta + \bar{B}_{2c} \cos 2\theta$ is very weak in the central region where the axisymmetric component B_{20} is mainly confined (figures 5*b*, 8). The evolution of vorticity q_2 is quite similar to that of Ψ_2 (see figure 7*b*), except that much stronger gradients develop in the vorticity field.

All these features can be easily understood if one represents (5.6*e*) in the form

$$\frac{\partial q_2}{\partial t} + \bar{\Omega}(r)\frac{\partial q_2}{\partial \theta} = -J(\Psi_1 + U_0 y - V_0 x, q_1 + y) - V_0. \tag{6.20}$$

By virtue of (5.11*b*) the residual streamfunction $\Psi_{res} = \Psi_1 + U_0 y - V_0 x$ is very small in the central region and the right-hand side of (6.20) is dominated here by the term $-V_0$ which contributes, obviously, to the development of an anticyclonic axisymmetric vortex (see figures 5*a*, *b*). In turn, the quadrupole part of the right-hand side is confined mainly to the vortex periphery characterized by a slow rotation rate, with the result that the vortex-satellite centres are practically immovable.

Since the extrema of the quadrupole harmonic amplitudes B_{2s} and B_{2c} are located at $r > 1$ the function $B_2(1, t)$ determining the patch shape distortion in (6.5*d*) is small: $|B_2(1, t)|$ does not exceed 2.5 for $t \leqslant 100$. Correspondingly, the correction term $\alpha^2(r_{2s}^{(2)} \sin 2\theta + r_{2c}^{(2)} \cos 2\theta)$ is non-zero at this order, but remains small.

7. The secondary β-gyres and translation speed correction

To determine the first non-zero correction U_2, V_2 to the translation speed we have to calculate the third-order fields. The equations for this approximation, being rather cumbersome in their full form, are greatly simplified by the relationships (5.7*a*), (6.6) and can be written as follows:

$$\nabla^2 \Psi_3 - \Psi_3 = q_3(r, \theta, t), \tag{7.1a}$$

$$[\Psi_3] = 0, \quad \left[\frac{\partial \Psi_3}{\partial r}\right] = -\bar{r}_3(\theta, t), \tag{7.1b}$$

$$\frac{\partial \bar{r}_3}{\partial t} + \bar{\Omega}(1)\frac{\partial \bar{r}_3}{\partial \theta} + \frac{\partial}{\partial \theta}\left[\bar{r}_2 \frac{\partial \Psi_{res}(1, \theta, t)}{\partial r} + \Psi_3(1, \theta, t)\right] + U_2 \cos\theta + V_2 \sin\theta = 0, \tag{7.1c}$$

$$\int_0^{2\pi} \bar{r}_3(\theta, t) \exp(\mathrm{i}\theta) \mathrm{d}\theta = 0. \tag{7.1d}$$

(*a*)

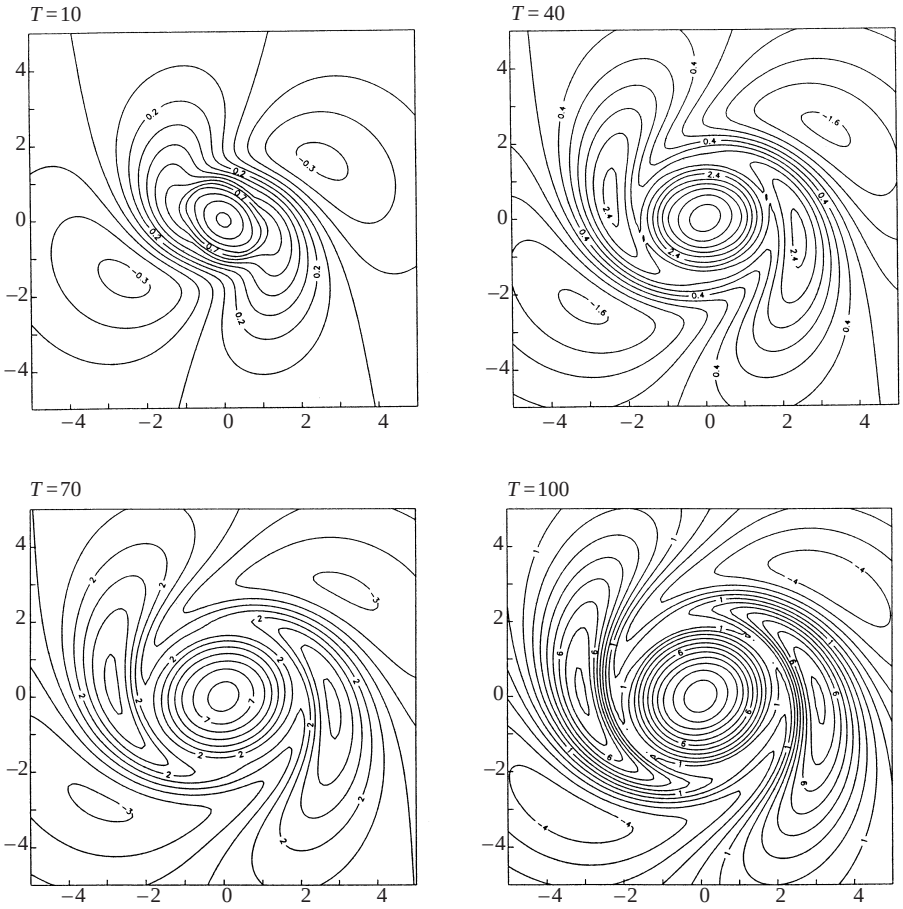

FIGURE 7(*a*). For caption see facing page.

The vorticity correction q_3 is obtained from (6.1*e*) and has the form

$$q_3 = n_{1s}\sin\theta + n_{1c}\cos\theta + n_{3s}\sin 3\theta + n_{3c}\cos 3\theta, \tag{7.2a}$$

$$n_1 = n_{1s} + \mathrm{i}n_{1c} = \mathrm{e}^{-\mathrm{i}\bar{\Omega}t}\int_0^t m\mathrm{e}^{\mathrm{i}\bar{\Omega}t}\mathrm{d}t, \tag{7.2b}$$

$$m = m_{qdr} + m_{ax}, \tag{7.2c}$$

$$m_{qdr} = \frac{1}{2r}[2(q_{2s} + \mathrm{i}q_{2c})\bar{A}^{*'} + (q_{2s} + \mathrm{i}q_{2c})'\bar{A}^{*} - 2\bar{B}_2\bar{Q}_1^{*'} - \bar{B}_2'\bar{Q}_1^{*}], \tag{7.2d}$$

$$m_{ax} = \frac{\mathrm{i}}{r}\left(q_{20}'\bar{A} - B_{20}'\bar{Q}_1\right). \tag{7.2e}$$

Here m_{qdr} and m_{ax} denote the contributions to the function m from the quadrupole and axisymmetrical components, respectively. Knowing q_3 one can find Ψ_3, r_3, and U_2, V_2 from (7.1*a*) to (7.1*d*). However the quantities U_2, V_2 which we are mainly interested in can be calculated in a simpler way.

(*b*)

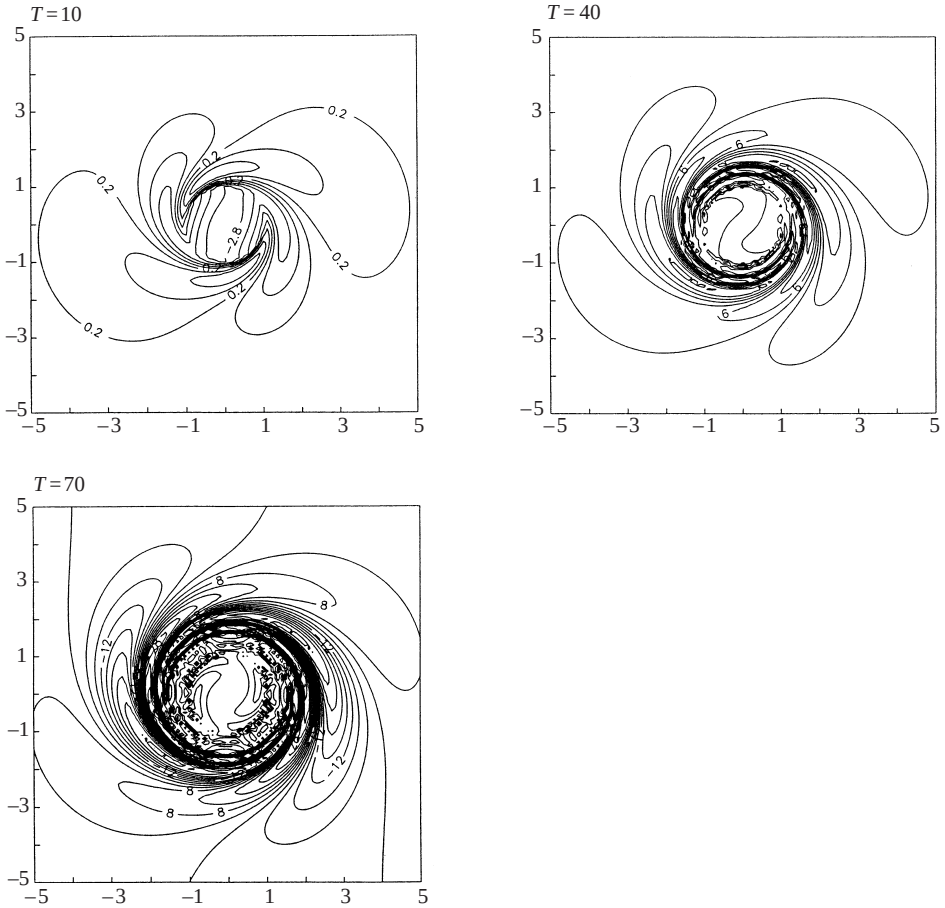

FIGURE 7. Time evolution of the second-order correction fields: (*a*) streamfunction $\Psi_2(r,\theta,t)$; (*b*) relative vorticity $q_2(r,\theta,t)$.

Let us represent the streamfunction Ψ_3 as a sum

$$\Psi_3 = \Psi_{q3} + \Psi_{H3}, \tag{7.3}$$

where Ψ_{q3} and Ψ_{H3} satisfy the equations

$$\nabla^2\Psi_{q3} - \Psi_{q3} = q_3, \quad [\Psi_{q3}] = \left[\frac{\partial\Psi_{q3}}{\partial r}\right] = 0, \tag{7.4}$$

$$\nabla^2\Psi_{H3} - \Psi_{H3} = 0, \ [\Psi_{H3}] = 0, \quad \left[\frac{\partial\Psi_{H3}}{\partial r}\right] = -\bar{r}_3. \tag{7.5}$$

The solution to (7.4) is given by the equations

$$\Psi_{q3} = \bar{b}_{1s}\sin\theta + \bar{b}_{1c}\cos\theta + \bar{b}_{3s}\sin 3\theta + \bar{b}_{3c}\cos 3\theta, \tag{7.6a}$$

$$\bar{b}_1(r,t) = \bar{b}_{1s} + \mathrm{i}\bar{b}_{1c} = -I_1(r)\int_r^\infty rn_1K_1(r)\mathrm{d}r - K_1(r)\int_0^r rn_1I_1(r)\mathrm{d}r. \tag{7.6b}$$

By virtue of (7.1*d*) the harmonics $\sin\theta$, $\cos\theta$ are absent from r_3 and, according to

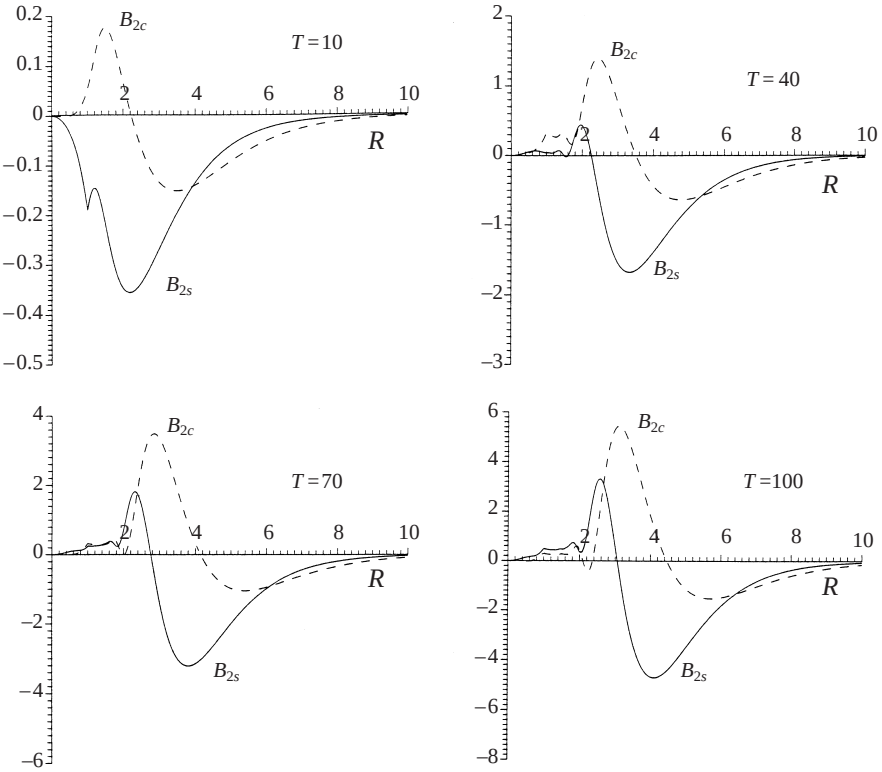

FIGURE 8. Radial profiles of the coefficients $\bar{B}_{2s}(r,t), \bar{B}_{2c}(r,t)$ in the quadrupole correction (see (6.4a)).

(7.5), also from Ψ_{H3}. Therefore using (7.6a,b), (5.7b), (6.4b) we have from (7.1c)

$$U_2 - \mathrm{i}V_2 = -\frac{\mathrm{i}}{2} R_2^{(2)} \bar{A}^{*\prime}(1,t) - \bar{b}_1(1,t), \tag{7.7a}$$

$$\bar{b}_1(1,t) = -I_1(1) \int_1^\infty r n_1 K_1(r)\mathrm{d}r - K_1(1) \int_0^1 r n_1 I_1(r)\mathrm{d}r. \tag{7.7b}$$

On the right-hand side of (7.7a) the first term is caused by the vortex patch distortion and the second term results from the dipole part of the streamfunction Ψ_3. The magnitude of $\bar{r}_2$ is small and the first term is found to be more than one order of magnitude smaller than the second. Thus we come to the conclusion that both the lowest-order translation speed $U_0 + \mathrm{i}V_0$ and the correction $U_2 + \mathrm{i}V_2$ are determined by the dipolar part of the field. In what follows the streamfunction Ψ_1 and the dipolar part of Ψ_3 will be referred to as the primary and the secondary β-gyres respectively.

The plots of U_2, V_2 as a function of t (figure 9a) reveal the strong variability of these quantities in time, both corrections U_2 and V_2 being predominantly positive. It means that the secondary β-gyres decelerate the vortex in the zonal direction and accelerate it in the meridional one. At the same time the modulus of the total translation speed $|\boldsymbol{U}_0 + \alpha^2 \boldsymbol{U}_2|$ is, on average, smaller than $|\boldsymbol{U}_0|$ (see figure 9b).

These effects, the meridional acceleration of the vortex along with its total deceleration, are clearly seen in figure 10 comparing the lowest-order and corrected tracks. Figure 10 is in a good qualitative agreement with analogous figure 4 of Sutyrin *et*

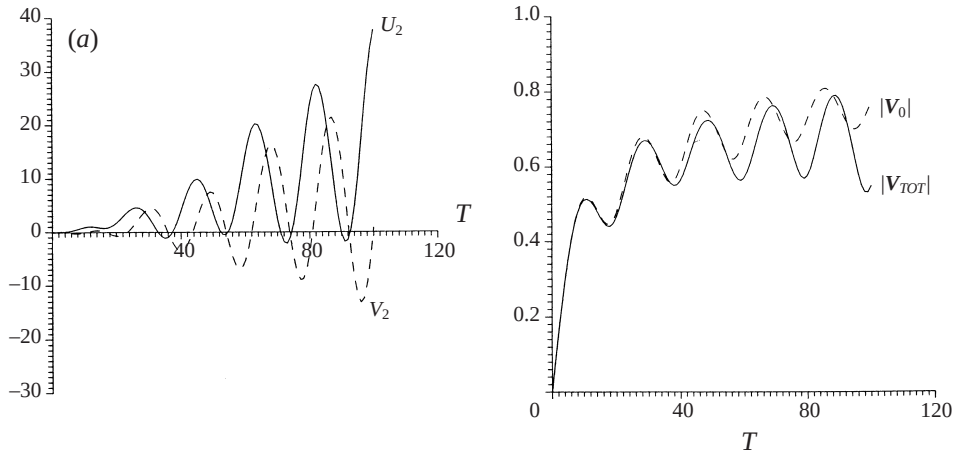

FIGURE 9. The translation speed correction: (*a*) U_2, V_2; (*b*) $|\boldsymbol{U}_0|$ (dashed line) and $|\boldsymbol{U}_0 + \alpha^2 \boldsymbol{U}_2|$ (solid line); $\alpha = 0.08$.

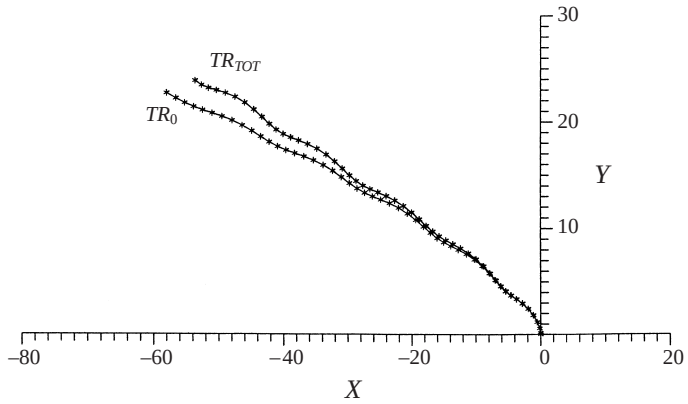

FIGURE 10. The vortex trajectories: TR_0 – the trajectory related to $\boldsymbol{U}_0$; TR_{TOT} – the corrected trajectory related to $\boldsymbol{U}_0 + \alpha^2 \boldsymbol{U}_2$; $\alpha = 0.08$.

al. (1994) which represents the lowest-order track produced by the primary β-gyres and the real vortex trajectories calculated numerically. However, Gaussian initial vortices were used in their paper; therefore one can hope that the effects described are common features of vortex dynamics on the β-plane.

Similarly to the case of U_0, V_0 (see figure 3 and its caption) the oscillatory behaviour of U_2, V_2 is related to the second term in the right-hand side of (7.7*b*) proportional to the integral over the vortex patch region. This is readily revealed when decomposing U_2, V_2 into the progressive (U_{2p}, V_{2p}) and the oscillatory (U_{2os}, V_{2os}) parts:

$$U_2 = U_{2P} + U_{2os}, \quad V_2 = V_{2P} + V_{2os}, \tag{7.8}$$

which result from the first and the second terms on the right-hand side of (7.7*b*) respectively. Figure 11 shows that only the component (U_{2p}, V_{2p}) makes a sign-definite contribution to the vortex track.

The evolution of the secondary β-gyres $\bar{b}_{1s} \sin\theta + \bar{b}_{1c} \cos\theta$ is shown in figure 12. At the initial stage the gyres look like a dipole approximately opposite in sign to the

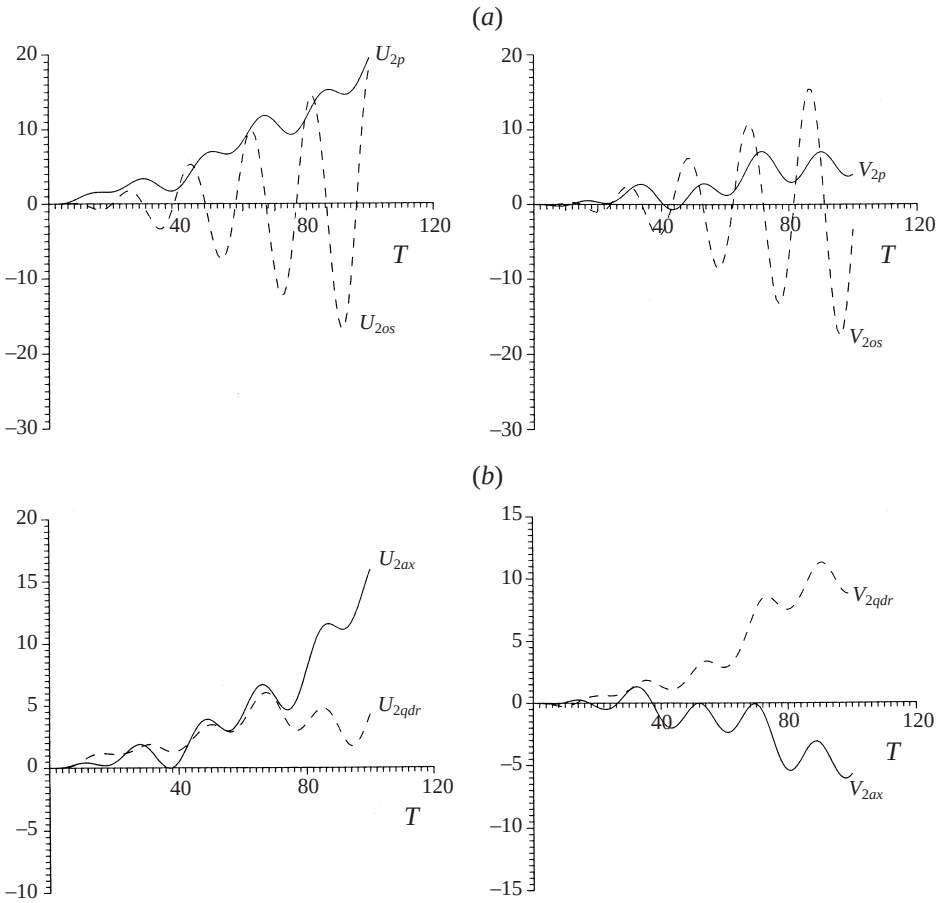

FIGURE 11. Analysis of various contributions to the translation speed correction (U_2, V_2): (*a*) decomposition of U_2, V_2 into the progressive and oscillatory parts; (*b*) decomposition of U_2, V_2 into the parts induced by the axisymmetrical (U_{2ax}, V_{2ax}) and quadrupole (U_{2qdr}, V_{2qdr}) parts of the second-order correction field. The oscillatory part is removed from the contribution due to the axisymmetric component.

primary β-gyres (compare figures 2 and 12 for $t = 10$). Also, like the primary β-gyres the magnitudes of the dipole vortices gradually grow in time and their centres migrate outward, along with a slow counterclockwise rotation decreasing as the centres move away from the main vortex centre. A new feature is that the vortex shapes change strongly in time; they elongate in the azimuthal direction bordering an approximately circular central region, also expanding with increasing time. The time variations in this region are much more rapid than in the bordering vortices.

Despite the more complicated structure, the mechanism of action of the secondary β-gyres is exactly the same as that of the primary ones. At each moment the configuration of the vortex centres correlates well with the signs of the components U_{2p}, V_{2p} as is seen when comparing figures 11 and 12. Thus the interaction between the dipole vortices makes a contribution to the progressive motion of the vortex; the rapid time changes in the central region produce only the oscillatory part (U_{2os}, V_{2os}) of the translation speed, which is unimportant dynamically despite its large amplitude.

The features of the secondary β-gyres are determined by the behaviour of the

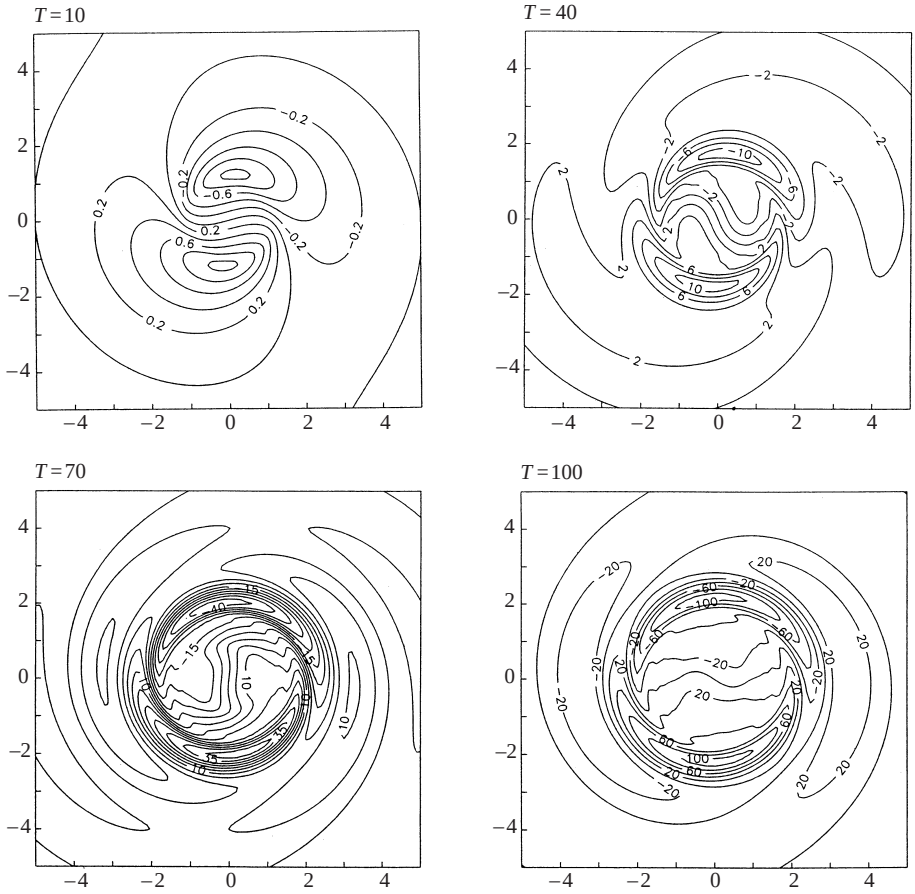

FIGURE 12. Time evolution of the secondary β-gyres.

right-hand side of (6.1*e*), which is conveniently rewritten as

$$\frac{\partial q_3}{\partial t} + \bar{\Omega}(r)\frac{\partial q_3}{\partial \theta} = R_{20\beta} + R_{201} + R_{221}, \tag{7.9}$$

where

$$R_{20\beta} = -\frac{\partial \Psi_{20}}{\partial x}, \tag{7.10}$$

$$R_{201} = -J(\Psi_{res}, q_{20}) - J(\Psi_{20}, q_1), \tag{7.11}$$

$$R_{221} = -J(\Psi_{res}, q_{qdr}) - J(\Psi_{qdr}, q_1) - \frac{\partial \Psi_{qdr}}{\partial x}. \tag{7.12}$$

The term $R_{20\beta}$ is the β-term part due to the axisymmetric correction Ψ_{20}; R_{201} represents the interaction between the axisymmetric component and the primary β-gyres; R_{221} is produced by the quadrupole fields,

$$\Psi_{qdr} = \bar{B}_{2s}\sin 2\theta + \bar{B}_{2c}\cos 2\theta, \quad q_{qdr} = q_{2s}\sin 2\theta + q_{2c}\cos 2\theta. \tag{7.13}$$

The contributions from the terms $R_{20\beta}$, R_{201}, and R_{221} to the secondary β-gyres behave in very different ways.

The contribution to the Ψ_3 field from the term $R_{20\beta}$ evolves in a manner similar

to the primary β-gyres, giving rise to a broad uniform flow in the central region advecting the vortex southwestward. Namely, this term produces a major part of the positive correction U_{2p} to the zonal translation speed. In turn the corresponding contribution from the term R_{201} results only in relatively fast oscillations in the vortex vicinity and contributes very little to the progressive vortex motion.

The streamfunction field produced by the quadrupole component (the term R_{221}), being a simple dipole at the initial stage, becomes in the course of time a complicated system consisting of intensifying vortices elongating in the azimuthal direction and being wound around an expanding approximately circular central region (not shown). Interaction between these vortices induces in the central region relatively weak almost rectilinear flow advecting the main vortex northward. Thus the quadrupole component produces an increase of the vortex meridional translation speed as is seen in figure 11(*b*).

Similarly to the case of the primary β-gyres the right-hand side of (7.9) multiplied by α^3 is a residual produced by the sum $\Psi_0 + \alpha\Psi_1 + \alpha^2\Psi_2$ being substituted into the vorticity equation. It is very important, therefore, that the right-hand side grows rather slowly in time. For example at $t = 100$ the right-hand-side amplitude does not exceed 60, i.e. the residual remains small even for the relatively low-amplitude case $\alpha = 0.08$. As in the case of the primary β-gyres this slow growth is caused by the structure of the fields Ψ_1, Ψ_2. The most rapid growth is related to the spatial gradients $\nabla q_1, \nabla q_2$, the strongest gradients being located approximately at the vortex core (see, for example, figure 5). In the Jacobian terms $J(\Psi_{res}, q_{20})$ and $J(\Psi_{res}, q_{qdr})$ these gradients are compensated by the smallness of Ψ_{res} in the central region (see § 5). In turn, the quadrupole streamfunction Ψ_{qdr}, being rather small in magnitude, is also located mainly outside the region of strong gradients of q_1 (see figure 8). This results in a slow growth of the Jacobian $J(\Psi_{qdr}, q_1)$. Finally, the term

$$J(\Psi_{20}, q_1) = \frac{1}{r}\frac{\partial \Psi_{20}}{\partial r}\frac{\partial q_1}{\partial \theta}$$

does not contain rapidly growing spatial derivatives.

Thus we see that the residual produced by the sum $\Psi_0 + \alpha\Psi_1 + \alpha^2\Psi_2$ remains small for relatively long times, at least up to $t = 100$ (100 advection times T_a). In the case $\alpha = 0.08$ (a typical value for the mid-oceanic eddies) the relative vorticity drops by approximately 18% by the time $t = 100$, i.e. this time is comparable to the distortion time T_d. Therefore the sum $\Psi_0 + \alpha\Psi_1 + \alpha^2\Psi_2$ can be a good approximation up to the distortion time T_d.

8. Discussion and conclusion

The mechanism of vortex deceleration somewhat resembles coupled wheels: the main vortex creates the primary β-gyres advecting the vortex along some trajectory; the primary β-gyres produce the axisymmetric and quadrupole corrections; the axisymmetric and quadrupole corrections together with the primary β-gyres induce the secondary β-gyres, decelerating the vortex motion and affecting its trajectory. All these processes ultimately result from the β-effect and proceed simultaneously, which makes a theoretical description of the vortex evolution a very complicated task. However, the problem is simplified in the case of an intense vortex where evolution is characterized by three well-separated time scales: the advective scale T_a, the wave scale T_w, and the distortion time T_d: $T_a \ll T_w \ll T_d$. The smallness of the parameter $\alpha = T_a/T_w$ allows us to seek the solution in the form of an asymptotic expansion

in terms of α. One might have expected the time of applicability of this expansion to be restricted to several advective times T_a, i.e. much smaller than the wave time T_w. However, our investigation shows that the first three terms of this asymptotic representation can serve as a good approximation for much longer times, at least up to $t = 100\,T_a$. For a moderate-amplitude vortex characterized by $\alpha = 0.08$ (the case of a mid-ocean eddy) the time $100\,T_a$ corresponds approximately to the destruction time T_d, i.e. the asymptotic representation can be a good approximation up to the stage of the vortex destruction.

The first stage of the vortex evolution, $t \leqslant T_w$, is dominated by the development of the β-gyres and other factors can be neglected. A gradual increasing of the β-gyre magnitude and size is accompanied by the rise of practically rectilinear uniform flow in the main vortex vicinity, intensifying and expanding with increasing time. Namely this flow advects the vortex along the dipole axis. Such a structure of the β-gyres in the vortex vicinity was clearly seen in all numerical experiments with intense isolated vortices (e.g. Fiorino & Elsberry 1989), and turns out to be of great importance, since it ultimately provides the applicability of the asymptotic solution for long times.

The enhancement of the β-gyres results in the amplification of the axisymmetric and quadrupole corrections. The axisymmetric correction is opposite (the same) in sign to the initial vortex in the vortex core (on the vortex periphery). Therefore in the course of time the axisymmetric vortex spreads out and decays. The rather complicated radial dependence of the azimuthally averaged relative vorticity given by the asymptotic theory is qualitatively the same as obtained in numerical experiments by Smith *et al.* (1995) with a Gaussian non-divergent vortex. Thus one might expect that such a structure is typical for vortex evolution on a β-plane. The energy and enstrophy of the axisymmetric component decrease practically linearly with respect to time with a rate directly proportional to α^2. Correspondingly, the typical lifetimes of a vortex obtained with use of the laws of energy and enstrophy conservation are directly proportional to the vortex streamfunction amplitude and inversely proportional to the squared Rossby wave group velocity βR_d^2. For the open-ocean eddies the typical lifetime turns out to be about 130 days, while for oceanic rings the corresponding lifetime is about 650 days.

Advection of the planetary vorticity by the axisymmetric and quadrupole components along with the nonlinear interaction of these components with the primary β-gyres produces the higher-order dipole circulation (so-called secondary β-gyres), affecting the vortex speed due to the primary β-gyres. As this takes place, the total speed and its zonal component decrease, whereas the meridional one increases, i.e. the vortex decelerates and deflects poleward. The zonal deceleration of the vortex is produced mainly by the advection of planetary vorticity by the axisymmetric correction (β-effect), and the meridional acceleration (which is also observed in numerical experiments) is due to the effect of the quadrupole component. These features were also clearly demonstrated in numerical experiment by Sutyrin *et al.* (1994) with Gaussian vortices.

The analysis of the primary β-gyres for $t \to \infty$ shows that the velocity of the almost uniform advecting flow in the vortex vicinity tends to the drift velocity of Rossby waves $-\beta R_d^2$. Thus, to leading order the system locally tends to the non-radiating state which is the sum of an axisymmetric vortex moving with the drift speed and of the uniform zonal flow having the same velocity. It is important that this tendency speeds up with increasing vortex amplitude. The existence of this tendency explains the so-called self-binding effect – the decreasing efficiency of wave radiation with increasing vortex amplitude – clearly demonstrated in numerical experiments by

Horton (1989), Smith & Reid (1982) *inter alia* (see also § 6). The secondary β-gyres retard this tendency and make it transient but their influence is weak for sufficiently long times for a large-amplitude vortex.

The above consideration leads us to the simple but important conclusion that the vortex translation speed and consequently the vortex track are determined by the dipolar component of the motion. This is clearly seen from the moment equations (3.8a, b) whose left-hand sides vanish in the absence of the dipolar component. Thus a correct description of the vortex dynamics is determined in many respects by the ability to describe correctly the behaviour of the β-gyres. In its turn this behaviour (at least for the divergent vortex) is determined mainly by near-field processes and is only slightly influenced by the far-field radiation up to rather large times.

The situation for a non-divergent vortex (which is of interest for atmospheric applications) is not so clear and calls for further investigation. The primary β-gyres induced in the vortex near field correctly describe the vortex evolution for times of the order of the wave time T_w. At the same time these β-gyres decay very slowly as $r \to \infty$, and the far-field Rossby wave radiation providing the correct behaviour of the solution at infinity is of importance even at the first order (Reznik & Dewar 1994; Llewellyn Smith 1997).

This work was supported by an ARC Small Grant, and RFBR grants 96-05-65209, 99-05-64841. G. M. R. gratefully acknowledges the hospitality of Monash University and University of Tasmania where the main part of the work was done. We are also grateful to Januscz Zuchowski and Mirek Szcap for their help in computational work.

Appendix

To derive the asymptotics of $A(r, t)$ for r fixed, $t \to \infty$ it is convenient to represent this function in the form

$$A = r - I_1(r)P_1 - I_1(r)P_2 - K_1(r)P_3, \tag{A 1}$$

where

$$P_1 = \int_{R_0}^{\infty} r^2 K_1(r) \mathrm{e}^{-\mathrm{i}\bar{\Omega}t} \mathrm{d}r, \quad P_2 = \int_{r}^{R_0} r^2 K_1(r) \mathrm{e}^{-\mathrm{i}\bar{\Omega}t} \mathrm{d}r, \quad P_3 = \int_{0}^{r} r^2 I_1(r) \mathrm{e}^{-\mathrm{i}\bar{\Omega}t} \mathrm{d}r, \tag{A 2}$$

and $R_0 \gg 1$. Using integration by parts one can readily show that

$$P_2 = O(1/t), \quad P_3 = O(1/t). \tag{A 3}$$

To estimate P_1 we rewrite it in terms of the new variable

$$b = \frac{K_1(r)}{r}. \tag{A 4}$$

Using the asymptotic of $K_1(r)$ for $r \gg 1$ (e.g. Gradshteyn & Ryzhik 1980) we obtain

$$P_1 \approx \int_0^{b_0} r^3(b) \mathrm{e}^{-\mathrm{i}b\tilde{t}} \mathrm{d}b \approx -\int_0^{b_0} \ln^3 b \mathrm{e}^{-\mathrm{i}b\tilde{t}} \mathrm{d}b, \tag{A 5}$$

where

$$b_0 = b(R_0), \quad \tilde{t} = I_1(1)t. \tag{A 6}$$

To estimate the integral

$$D = -\int_0^{b_0} \ln^3 b \mathrm{e}^{-\mathrm{i}b\tilde{t}} \mathrm{d}b, \tag{A 7}$$

we represent it in the form

$$D = -\frac{1}{\tilde{t}}\int_0^{b_0\tilde{t}} \ln^3\frac{u}{\tilde{t}}\mathrm{e}^{-\mathrm{i}u}\mathrm{d}u = -\frac{1}{\tilde{t}}\int_0^{b_0\tilde{t}} (\ln^3 u - 3\ln^2 u\ln\tilde{t} + 3\ln u\ln^2\tilde{t} - \ln^3\tilde{t})\mathrm{e}^{-\mathrm{i}u}\mathrm{d}u, \tag{A 8}$$

and use the asymptotic formula

$$\int_0^s \mathrm{e}^{\mathrm{i}x}\ln^n x\mathrm{d}x = -\mathrm{i}\mathrm{e}^{\mathrm{i}s}\ln^n s + C_n + O\left(\frac{\ln^{n-1} s}{s}\mathrm{e}^{\mathrm{i}s}\right), \quad s\to\infty, \tag{A 9}$$

$$C_n = \mathrm{i}n\int_1^\infty \frac{\ln^{n-1} x}{x}\mathrm{e}^{\mathrm{i}x}\mathrm{d}x + \int_0^1 \mathrm{e}^{\mathrm{i}x}\ln^n x\mathrm{d}x, \quad n>0.$$

As a result we have

$$P_1 \approx D = -G(\tilde{t}), \tag{A 10}$$

whence (5.12*a*) follows.

To derive the asymptotic formula (5.10*a*, *b*) for $u = \bar{\Omega}(r)t$ fixed, $t\to\infty$ we represent A in the form

$$A = r - I_1(r)\bar{P}_1 - K_1(r)\bar{P}_2 - K_1(r)\bar{P}_3, \tag{A 11}$$

where

$$\bar{P}_1 = \int_r^\infty r^2 K_1(r)\mathrm{e}^{-\mathrm{i}\bar{\Omega}t}\mathrm{d}r; \quad \bar{P}_2 = \int_0^{R_0} r^2 I_1(r)\mathrm{e}^{-\mathrm{i}\bar{\Omega}t}\mathrm{d}r; \quad \bar{P}_3 = \int_{R_0}^r r^2 I_1(r)\mathrm{e}^{-\mathrm{i}\bar{\Omega}t}\mathrm{d}r. \tag{A 12}$$

One can readily obtain that

$$\bar{P}_1 \sim \int_0^b r^3(b)\mathrm{e}^{-\mathrm{i}b\tilde{t}}\,\mathrm{d}b \approx -\int_0^b \mathrm{e}^{-\mathrm{i}b\tilde{t}}\ln^3 b\mathrm{d}b = -\frac{1}{\tilde{t}}\int_0^u \mathrm{e}^{-\mathrm{i}v}\,\ln^3\frac{v}{\tilde{t}}\mathrm{d}v$$

$$= \frac{\ln^3\tilde{t}}{\tilde{t}}\int_0^u \mathrm{e}^{-\mathrm{i}v}\mathrm{d}v + O(\ln^2\tilde{t}/\tilde{t}),$$

so that

$$\bar{P}_1 = \frac{\ln^3\tilde{t}}{\tilde{t}}\mathrm{i}(\mathrm{e}^{-\mathrm{i}x} - 1) + O\left(\frac{\ln^2\tilde{t}}{\tilde{t}}\right). \tag{A 13}$$

Using the asymptotic formula

$$I_1(r) \sim \frac{1}{2b\ln^2 b}, \quad r\to\infty, \tag{A 14}$$

we write $\bar{P}_3$ as

$$\bar{P}_3 = \int_{R_0}^r r^2 I_1(r)\mathrm{e}^{-\mathrm{i}b\tilde{t}}\,\mathrm{d}r \sim \int_b^{b_0} \frac{\mathrm{e}^{-\mathrm{i}b\tilde{t}}}{2b^2}\mathrm{d}b = \frac{\tilde{t}}{2}\int_u^{b_0\tilde{t}} \frac{\mathrm{e}^{-\mathrm{i}v}}{v^2}\mathrm{d}v,$$

whence

$$\bar{P}_3 = \frac{\tilde{t}}{2}\int_u^\infty \frac{\mathrm{e}^{-\mathrm{i}v}}{v^2}\mathrm{d}v + O(1/\tilde{t}). \tag{A 15}$$

Finally, one can readily show that

$$\bar{P}_2 = O(1/t). \tag{A 16}$$

Using (A 13), (A 14), (A 15), (A 16) and the equations

$$K_1(r) = \frac{r}{\tilde{t}}\frac{K_1(r)}{r}\tilde{t} = \frac{ru}{\tilde{t}}, \quad r = \ln\tilde{t} + O(1) \quad \text{for } u \text{ fixed}, \quad t \to \infty \tag{A 17}$$

we obtain (5.10*a*, *b*).

REFERENCES

Fiorino, M. & Elsberry, R. L. 1989 Some aspects of vortex structure related to tropical cyclone motion. *J. Atmos. Sci.* **46**, 975.

Firing, E. & Beardsley, R. 1976 The behaviour of a barotropic eddy on a β-plane. *J. Phys. Oceanogr.* **6**, 57.

Flierl, G. R. 1977 The application of linear quasi-geostrophic dynamics to Gulf Stream rings. *J. Phys. Oceanogr.* **7**, 365.

Flierl, G. R. 1984 Rossby wave radiation from a strongly nonlinear warm eddy. *J. Phys. Oceanogr.* **14**, 47.

Flierl, G. R. & Haines, K. 1994 The decay of modons due to Rossby wave radiation. *Phys. Fluids* **6**, 3487.

Gradshteyn, I. S. & Ryzhik, I. M. 1980 *Table of Integrals, Series, and Products*, 2nd Edn. Academic.

Horton, W. 1989 Drift wave vortices and anomalous transport. *Phys. Fluids* B **1**, 524.

Korotaev, G. K. 1988 *Theoretical Modelling of Synoptical Variability of the Ocean.* Kiev: Naukova Dumka (in Russian).

Korotaev, G. K. & Fedotov, A. B. 1994 Dynamics of an isolated barotropic eddy on a β-plane. *J. Fluid Mech.* **264**, 277.

Llewellyn Smith , S. G. 1997 The motion of a non-isolated vortex on the beta-plane. *J. Fluid Mech.* **346**, 149.

McDonald, N. R. 1998 The decay of cyclonic eddies by Rossby wave radiation, *J. Fluid Mech.* **361**, 237.

McWilliams, J. C. & Flierl, G. R. 1979 On the evolution of isolated, nonlinear vortices. *J. Phys. Oceanogr.* **9**, 1155.

Mied, R. P. & Lindemann, G. J. 1979 The propagation and evolution of cyclonic Gulf Stream rings. *J. Phys. Oceanogr.* **9**, 1183.

Reznik, G. M. 1992 Dynamics of singular vortices on a beta-plane. *J. Fluid Mech.* **240**, 405.

Reznik, G. M. & Dewar, W. K. 1994 An analytical theory of distributed axisymmetric barotropic vortices on the β-plane. *J. Fluid Mech.* **269**, 301.

Reznik, G. M., Grimshaw, R. H. J. & Sriskandarajah, K. 1997 On the evolution of two-layer localised quasigeostrophic vortices on a β-plane. *Geophys. Astrophys. Fluid Dyn.* **86**, 1–42.

Ross, R. J. & Kurihara, Y. 1992 A simplified scheme to simulate asymmetries due to the β effect in barotropic vortices. *J. Atmos. Sci.* **49**, 1620.

Smith, D. C. & Reid, H. O. 1982 A numerical study of nonfrictional decay of mesoscale eddies. *J. Phys. Oceanogr.* **12**, 244.

Smith, R. K., Weber, H. C. & Kraus, A. 1995 On the symmetric circulation of a moving hurricane. *Q. J. R. Metl. Soc.* **121**, 945.

Sutyrin, G. G. & Flierl, G. R. 1994 Intense vortex motion on the beta plane: development of the beta gyres. *J. Atmos. Sci.* **51**, 773.

Sutyrin, G. G., Hesthaven, J. S., Lynov, J. P. & Rasmussen, J. J. 1994 Dynamical properties of vortical structures on the beta-plane. *J. Fluid Mech.* **268**, 103.

Sutyrin, G. G. & Morel 1997 Intense vortex motion in a stratified fluid on the beta-plane: an analytical theory and its validation. *J. Fluid Mech.* **336**, 203.